

Supporting Information

Oxidative *N*-Formylation of Secondary Amines Catalyzed by Reusable Bimetallic AuPd–Fe₃O₄ Nanoparticles

Sabyuk Yang, Ahra Cho [†], Jin Hee Cho [†] and Byeong Moon Kim ^{*}

Department of Chemistry, College of Natural Sciences, Seoul National University, Seoul 08826, Korea;

diablopkpk@snu.ac.kr (S.Y.); araelliecho@snu.ac.kr (A.C.); 201722658@snu.ac.kr (J.H.C.)

^{*} Correspondence: kimbm@snu.ac.kr

[†] These authors contributed equally to this work.

Table of Contents

I. Experimental section

1. General information.....	S3
2. Experimental procedures of the synthesis of catalysts.....	S8
3. Supplementary reaction optimization data	
• Table S1. Catalyst screening.....	S10
• Table S2. Base screening.....	S11
• Table S3. Catalyst loading.....	S12
4. Characterization of catalysts	
• Figure S1. SEM analysis.....	S13
• Figure S2. SEM-EDS analysis.....	S14
• Figure S3. EDS map spectrum.....	S17
• Figure S4. HR-TEM analysis.....	S18
• Figure S5. BF-STEM and HADDF-STEM analysis.....	S20
• Figure S6. Particle distribution of AuPd–NPs.....	S22
• Figure S7. XPS analysis.....	S24
• Figure S8. ICP-AES analysis.....	S26
• Figure S9. XRD analysis.....	S27

5. Supplementary data	
• Figure S10. SEM, EDS, and ICP-AES analysis of $\text{Au}_x\text{Pd}_y\text{-Fe}_3\text{O}_4$	S28
• Figure S11. SEM analysis of recycled catalyst.....	S32
• Figure S12. HR-TEM analysis of recycled catalyst.....	S33
• Figure S13. SEM analysis of other AuPd–NPs.....	S34
• Table S4. ICP-AES of other AuPd–NPs.....	S34
• Table S5. Formylation data with other AuPd–NPs.....	S35
• Figure S14. Kinetic data of <i>N</i> -formylation.....	S35
• Table S6. Substrate scope under high substrate concentration.....	S36
• Figure S15. Determination of the methanol oxidation products.....	S37
• Figure S16. Initial kinetics of methanol oxidation to HCHO as measured from HCHO-DNPH generation.....	S38
• Table S7. Control experiments.....	S39
6. Characterization of products.....	S40
 II. References.....	 S48
III. NMR spectra.....	S49

I. Experimental section

1. General information

All 1D NMR spectroscopy experiments were conducted with a DD2MR400 (Agilent Technologies, Santa Clara, CA, USA) for 400 MHz, Varian 500 (Varian, Inc., Palo Alto, CA, USA) for 500 MHz. NMR spectra were processed with MestReNova. Chemical shifts are reported in ppm and referenced to residual solvent peaks (CHCl_3 in CDCl_3 : 7.26 ppm for ^1H , 77 ppm for ^{13}C). Coupling constants are reported in Hertz. Secondary amine substrates (**1b**, **1d**, **1e**, **1f**, **1i**, **1k**, **1l**, **1m**, **1q**) were synthesized by known procedures.^[1–3] Rest of the starting materials and reagents were purchased from Acros Organics (Pittsburgh, PA, USA), Sigma-Aldrich Aldrich (St. Louis, MO, USA), Alfa Aesar (Ward Hill, MA, USA), Tokyo Chemical Industry (Tokyo, Japan), and used without further purification.

Catalyst characterization

SEM images were obtained using JSM-7800F Prime (JEOL Ltd., Tokyo, Japan). HR-TEM images were obtained using JEM-3010 (JEOL Ltd., Tokyo, Japan). STEM images were obtained using JEM-ARM200F (JEOL Ltd., Tokyo, Japan). XPS data were obtained using AXIS SUPRA (Kratos Analytical Ltd., Manchester, UK). ICP-AES data were obtained using OPTIMA 8300 (Perkin-Elmer, Waltham, MA, USA). The machines mentioned above are installed at the National Center for Inter-University Research Facilities (NCIRF) at Seoul National University.

The powder X-ray diffraction (XRD) was performed using a D8 Advance (Bruker, Billerica, MA, USA) installed the National Instrumentation Center for Environmental Management (NICEM) at Seoul National University.

Materials/Instrumentation

ESCA (Electron Spectroscopy for Chemical Analysis)

1. Model: AXIS SUPRA (Kratos Analytical Ltd., Manchester, UK)

2. Vacuum System

(1) The sample analysis chamber is a multiport ultra-high vacuum chamber of mu-metal construction.

(2) Bakeout: 24 hours~7 day timer with thermostatically controlled, no need remove any cables and cameras before baking.

(3) Pumping kit

- The sample analysis chamber: TMP, TSP

- (Base pressure in the analysis chamber is $< 5 \times 10^{-10}$ torr)

- The load lock chamber: TMP, oil free dry scroll pump.

- (Base pressure in the analysis chamber is $< 5 \times 10^{-8}$ torr)

3. Electron energy analyzer

(1) 165 mm mean radius concentric hemispherical analyzer for spectroscopy and a spherical mirror analyzer for imaging.

(2) 128 channel delay line detector (DLD) be used for both spectroscopy and parallel imaging modes.

(3) In spectroscopy mode should have greater than 100 discrete data channels improving the sensitivity in spectroscopy mode.

(4) X-ray photoelectron spectroscopy

- Ultimate energy resolution: ≤ 0.48 eV (Ag3d_{5/2} peak)

(5) X-ray photoelectron imaging

- Lateral resolution of the parallel imaging: $\leq 1 \mu\text{m}$

4. Automated monochromatic X-ray source

(1) 500 mm Rowland circle geometry, controlled by data system.

(2) Auto arrangement provides easy control, optimization and calibration of the mirror

position and ensures that the X-ray illuminated area is correctly aligned with the analysis position.

5. Sample alignment system

- (1) Load lock chamber camera gives a global view of each sample holder such that analysis positions can be viewed, indexed and pre-programmed ready for data acquisition.
- (2) High magnification sample analysis chamber microscope has a motorized, more than 12 x optical zoom controlled from the data-system facilitating remote operation of the camera.
- (3) The optical images are captured within the Data Acquisition software and should be saved and manipulated in the Data Processing software.

6. Sample manipulator and platen

- (1) Automated five axis X, Y, Z, Θ , Φ precision manipulator system

X-axis; 150 mm

Y-axis; ± 15 mm

Z-axis; -12~+16 mm

Θ -rotation; $\pm 90^\circ$

Φ -rotation; $\pm 180^\circ$

- (2) The sample manipulator have standard reference materials (Au, Ag and Cu) for spectroscopic calibration as well as an Au grid for imaging calibration permanently mounted.
- (3) sample holder: Dual height sample holder, Combination sample holder, Z-rotation sample holder

7. Gas cluster ion source

- (1) Monatomic Ar^+ ion mode: 500 eV ~ 5 keV
- (2) Ar^{n+} cluster ion mode: ~ 20 keV
- (3) The ion source be fully integrated with the data acquisition system.

8. UPS (Ultraviolet Photoelectron Spectroscopy)

- (1) Windowless discharge lamp of fully bakeable metal and ceramic construction
- (2) The minimum step size: 1 meV
- (3) Sensitivity: 1,000,000 cps at 120 meV resolution
 - Ag Fermi edge excited by He I radiation
- (4) He I: He II ratio: 4 : 1

9. ISS (Ion Scattering Spectroscopy)

- (1) Ion scattering spectroscopy: Ar⁺ or He⁺ ions.
- (2) Energy resolution
 - Sensitivity: 12,000 cps/nA at 12 eV FWHM
 - Au scattering, 1 kV He⁺ ions

Transmission Electron Microscope II (ccd camera type)

- 1. Model: JEM-3010 (JEOL Ltd., Tokyo, Japan)
- 2. Accelerating Voltage: 80 to 300 Kv
- 3. Gatan Digital Camera (MSC-794)
- 4. Resolution: Point image: 0.17 nm
 - Lattice image: 0.14 nm
- 5. MAG: x50 ~ x1,500,000
- 6. Camera Length: SA DIFF Mode: 120 ~ 3,000 mm

Cs-STEM (Cs corrected STEM with Cold FEG)

- 1. Model: JEM-ARM200F (JEOL Ltd., Tokyo, Japan)
- 2. Specifications
 - a. HT: 60, 80, 120, 200 kV
 - b. Magnification: 50 to 2,000,000 X (TEM), 200 to 1,500,000 X (STEM)
 - c. Resolution

- STEM mode: HAADF 0.08 nm/ BF 0.136 nm

- TEM mode: Point 0.23 nm

d. Sample tilting

- X / Y: $\pm 35^\circ$ / $\pm 30^\circ$

3. Analysis functions

a. CCD Camera: OneView camera (25 fps at full 4k x 4k resolution)

b. EDS: SDD Type (Active area 100mm²/ Solid angle 0.9 sr)

c. EELS: Model 965 GIF Quantum ER

2. Experimental procedures of the synthesis of catalysts

Synthesis of AuPd–Fe₃O₄ NPs

Initially, 177 mg of PdCl₂ and 2.00 g of PVP (M_w~10,000 mg mol⁻¹) were placed in 40 mL of ethylene glycol (EG) in a 100 mL round-bottom flask. This mixture was sonicated for 10 min and stirred for 1 h at 100 °C in an oil bath. In a separate 100 mL round-bottom flask, 390 mg of HAuCl₄·3H₂O and 1.00 g of PVP were added to 40 mL of water in a 100 mL round-bottom flask. This mixture was sonicated for 10 min and stirred for 30 min at 60 °C in an oil bath. Meanwhile, 1.00 g of Fe₃O₄ NPs were added to 300 mL of water in a two-necked 500 mL round-bottom flask and then sonicated for 10 min. The prepared Pd precursor solution was then injected dropwise onto the Fe₃O₄ suspension with vigorous stirring. After 5 min, the Au precursor solution was added and 100 mg of sodium borohydride in 40 mL of water was injected dropwise using a syringe pump. The resulting mixture was stirred for 5 h at 60 °C. Subsequently, the AuPd alloy on Fe₃O₄ nanoparticles was retrieved via sonication and washing with ethanol (40 mL x 10 times) and dried on a rotary evaporator to give AuPd–Fe₃O₄ NPs (950 mg, 95% yield).

Synthesis of Au–Fe₃O₄ NPs

Initially, 39 mg of HAuCl₄·3H₂O and 100 mg of PVP were placed in 4.0 mL of water in a 10 mL round-bottom flask. This solution was sonicated for 1 min and stirred for 30 min at 60 °C. Meanwhile, 100 mg of Fe₃O₄ NPs was added to 30 mL of water in a two-necked 100 mL round-bottom flask. The prepared precursor solution was then injected dropwise to Fe₃O₄ NPs in 30 mL of water, followed by dropwise addition of 10 mg of sodium borohydride in 4.0 mL of water. The mixture was stirred at 60 °C for an additional 5 h. The resultant product was washed with ethanol (40 mL x 10 times) and dried on a rotary evaporator to give Au–Fe₃O₄ NPs (94.8 mg, 95% yield).

Synthesis of Pd–Fe₃O₄ NPs

Initially, 177 mg of PdCl₂ and 2.00 g of PVP were placed in 40 mL of EG in a 100 mL round-bottom flask. This mixture was sonicated for 10 min and stirred for 1 h at 100 °C. Meanwhile, 500 mg of Fe₃O₄ NPs was added to 150 mL of EG in a two-necked 500 mL round-bottom flask. The prepared precursor solution was then injected dropwise to Fe₃O₄ NPs in 150 mL of EG, and stirred at 100 °C for an additional 24 h. The resultant product was washed with ethanol (40 mL x 10 times) and dried on a rotary evaporator to give Pd–Fe₃O₄ NPs (440.0 mg, 88% yield).

Synthesis of Au_xPd_y–Fe₃O₄ NPs

For Au_xPd_y–Fe₃O₄ synthesis, the same method used for the synthesis of AuPd–Fe₃O₄ NPs was employed, with different quantities of metals and sodium borohydride. To prepare Au₁Pd_{0.23}–Fe₃O₄ NPs, PdCl₂ (0.011 g) with PVP (0.125 g), HAuCl₄·3H₂O (0.098 g) with PVP (0.250 g), and sodium borohydride (0.025 g) were used. For the synthesis of Au₁Pd_{0.39}–Fe₃O₄ NPs, PdCl₂ (0.022 g) with PVP (0.250 g), HAuCl₄·3H₂O (0.098 g) together with PVP (0.250 g), and sodium borohydride (0.025 g) were used. In the case of Au_{0.65}Pd₁–Fe₃O₄ NPs, PdCl₂ (0.044 g) with PVP (0.500 g), HAuCl₄·3H₂O (0.049 g) with PVP (0.125 g), and sodium borohydride (0.013 g) were used. Finally, for the preparation of Au_{0.39}Pd₁–Fe₃O₄ NPs, PdCl₂ (0.044 g) with PVP (0.500 g), HAuCl₄·3H₂O (0.033 g) with PVP (0.083 g), and sodium borohydride (0.008 g) were used. The resulting mixture was stirred for 5 h at 60 °C. Subsequently, the Au_xPd_y alloy on Fe₃O₄ nanoparticles was retrieved via sonication and washing with ethanol (40 mL x 10 times) and dried on a rotary evaporator to give Au₁Pd_{0.23}–Fe₃O₄ NPs (85.6 mg, 86% yield), Au₁Pd_{0.39}–Fe₃O₄ NPs (80.6 mg, 81% yield), Au_{0.65}Pd₁–Fe₃O₄ NPs (99.9 mg, >99% yield), and Au_{0.39}Pd₁–Fe₃O₄ NPs (89.6 mg, 90% yield).

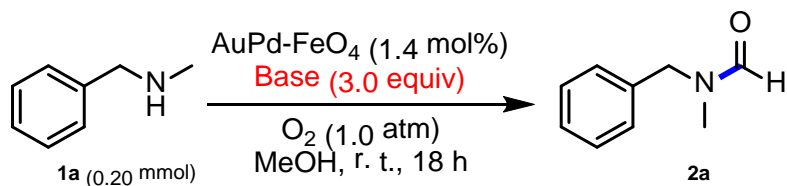
3. Supplementary reaction optimization data

Table S1. Catalyst screening^a

<p> <chem>CN(C)Cc1ccccc1</chem> (1a, 0.20 mmol) $\xrightarrow[\text{MeOH, r. t., 18 h}]{\text{Catalyst (x mol\%), NaOH (3.0 equiv), O}_2 \text{ (1.0 atm)}}$ <chem>CN(C)C=O</chem> (2a) </p>		
Entry	Catalyst (mol%)	Yield (%) ^b
1	Fe ₃ O ₄ (1.4)	Not detected
2	Au–Fe ₃ O ₄ (2.8)	25
3	Pd–Fe ₃ O ₄ (2.8)	55
4	Au–Fe ₃ O ₄ (1.4) + Pd–Fe ₃ O ₄ (1.4)	91
5	AuPd–Fe ₃ O ₄ (1.4)	65
6	PdPt–Fe ₃ O ₄ (2.0)	21

^a Reaction conditions: *N*-methyl-1-phenylmethanamine (0.20 mmol), catalyst (x mol%) NaOH (3.0 equiv), methanol (1.0 mL), O₂ (1.0 atm), r. t., 18 h.

^b Determined from ¹H NMR spectral analysis through the use of mesitylene as an internal standard.

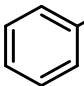
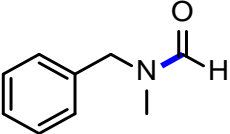
Table S2. Base screening^a

Entry	Base	Yield (%) ^b	Entry	Base	Yield (%) ^b
1	-	14	9	K_2CO_3	54
2	$\text{LiOH}\cdot\text{H}_2\text{O}$	60	10	Cs_2CO_3	69
3	NaOH	65	11	NaOtBu	59
4	KOH	75	12	KOtBu	69
5	$\text{RbOH}\cdot x\text{H}_2\text{O}$	74	13	K_2HPO_4	3
6	$\text{CsOH}\cdot\text{H}_2\text{O}$	91	14	K_3PO_4	60
7	Li_2CO_3	20	15	NaOAc	19
8	Na_2CO_3	29	16	CsF	39

^a Reaction conditions: *N*-methyl-1-phenylmethanamine (0.20 mmol), $\text{AuPd-Fe}_3\text{O}_4$ (1.4 mol%), base (3.0 equiv), methanol (1.0 mL), O_2 (1.0 atm), r. t., 18 h.

^b Determined from ^1H NMR spectral analysis through the use of mesitylene as an internal standard.

Table S3. Catalyst loading^a

<div><div><div><div></div><div>1a (0.20 mmol)</div></div><div><div><div>$\xrightarrow[\text{MeOH, r. t., 18 h}]{\text{AuPd-Fe}_3\text{O}_4 \text{ (x mol\%)} \atop \text{CsOH}\cdot\text{H}_2\text{O (3.0 equiv)} \atop \text{O}_2 \text{ (1.0 atm)}}$</div><div></div></div><div><div><div></div><div>2a</div></div></div></div></div></div>			
Entry	Catalyst loading (mol%)	TON ^b	Yield (%) ^c
1	0.4	89	71
2	0.7	50	70
3	1.1	35	78
4	1.4	33	91
5	1.8	24	85
6	2.1	20	83

^a Reaction conditions: *N*-methyl-1-phenylmethanamine (0.20 mmol), AuPd-Fe₃O₄ (x mol%), CsOH·H₂O (3.0 equiv), methanol (1.0 mL), O₂ (1.0 atm), r. t., 18 h.

^b Turnover number (TON)=mmol of product/mmol of metal

^c Determined from ¹H NMR spectral analysis through the use of mesitylene as an internal standard.

3. Characterization of Catalysts

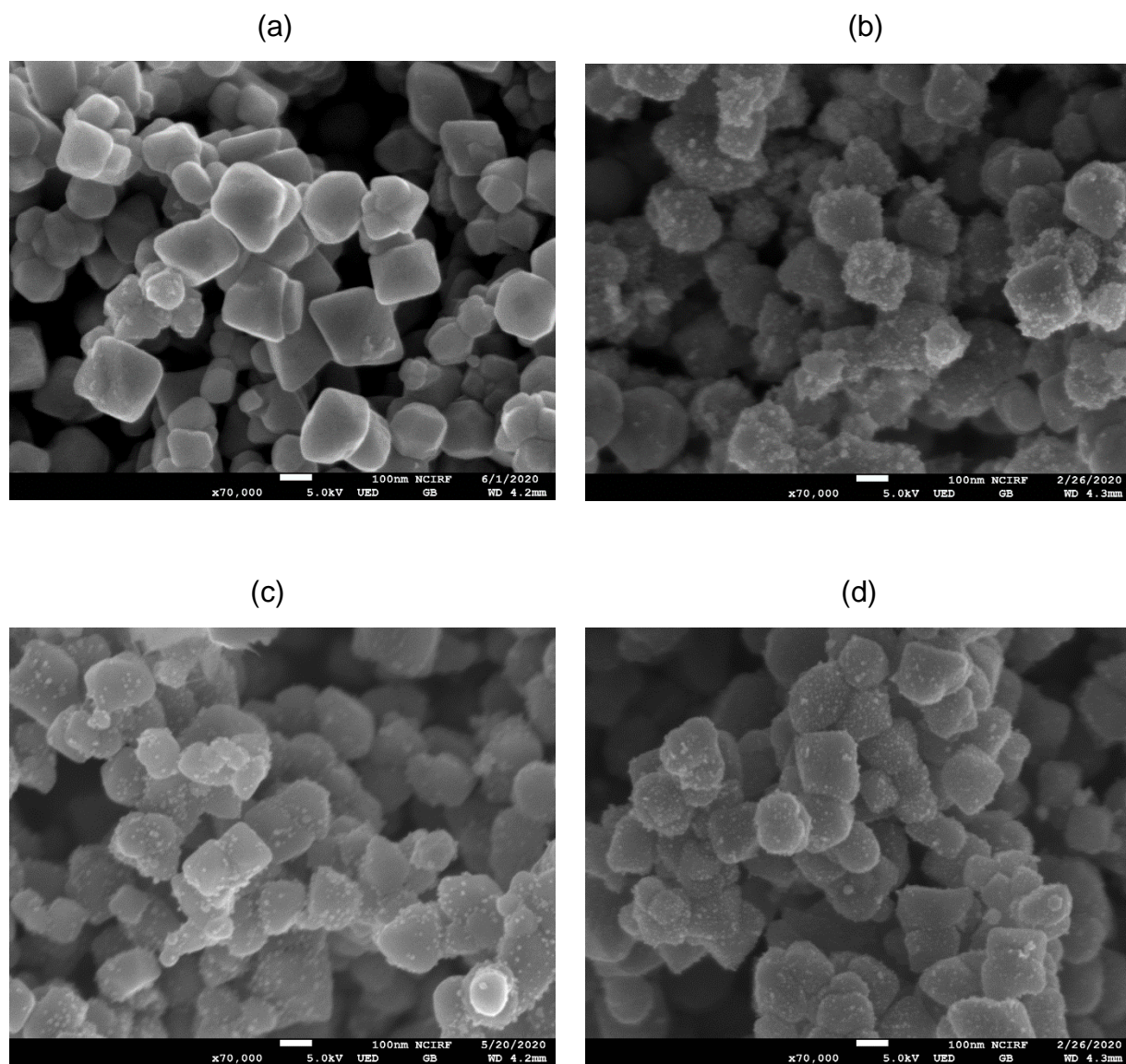
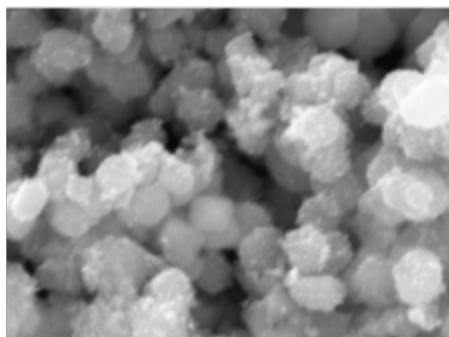


Figure S1. SEM image of (a) Fe₃O₄ NPs, (b) AuPd-Fe₃O₄ NPs, (c) Au-Fe₃O₄ NPs, and (d) Pd-Fe₃O₄ NPs

(a)

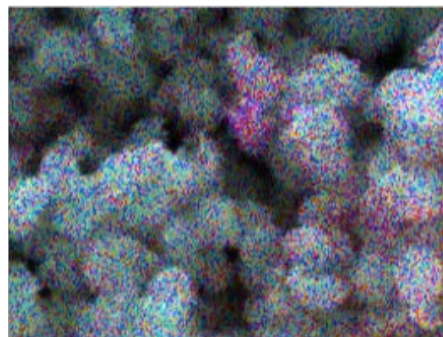
Electron Image 3



500nm

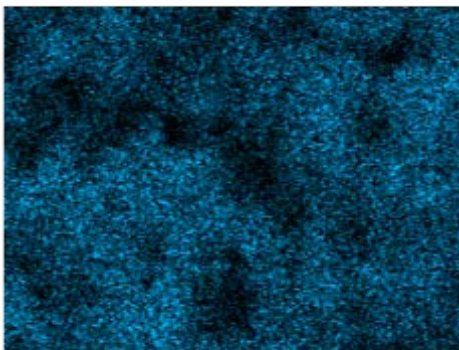
(b)

EDS Layered Image 2



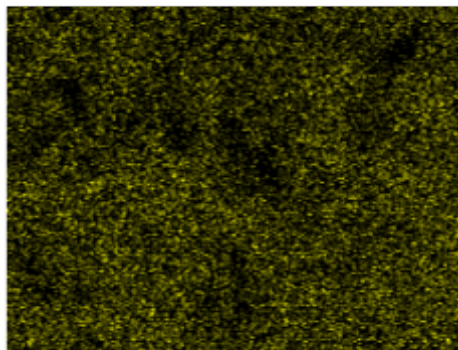
500nm

O K series



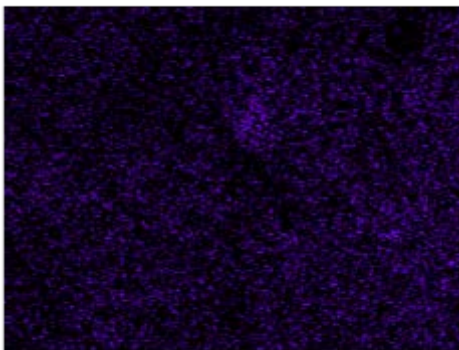
500nm

Fe K series



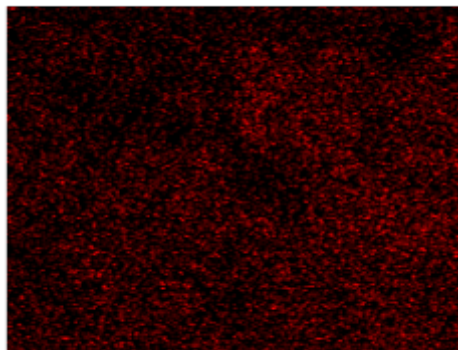
500nm

Pd L series



500nm

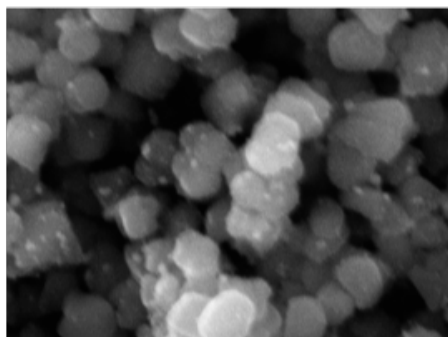
Au M series



500nm

(c)

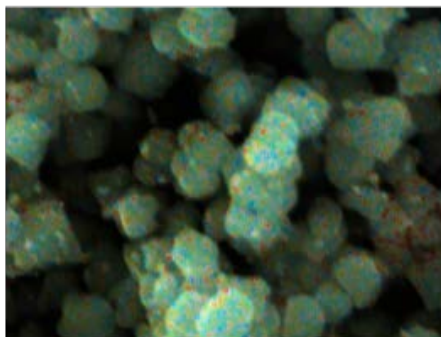
Electron Image 4



500nm

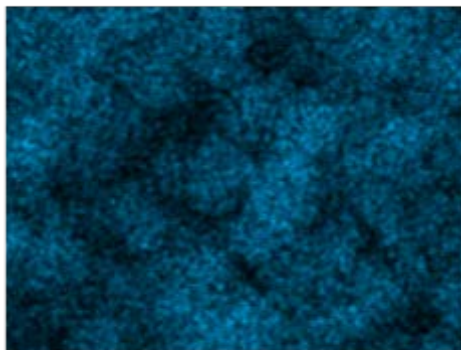
(d)

EDS Layered Image 4



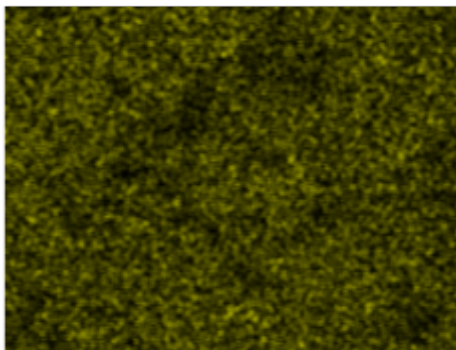
500nm

O K series



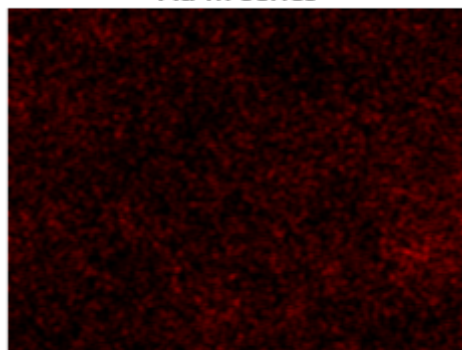
500nm

Fe K series



500nm

Au M series



500nm

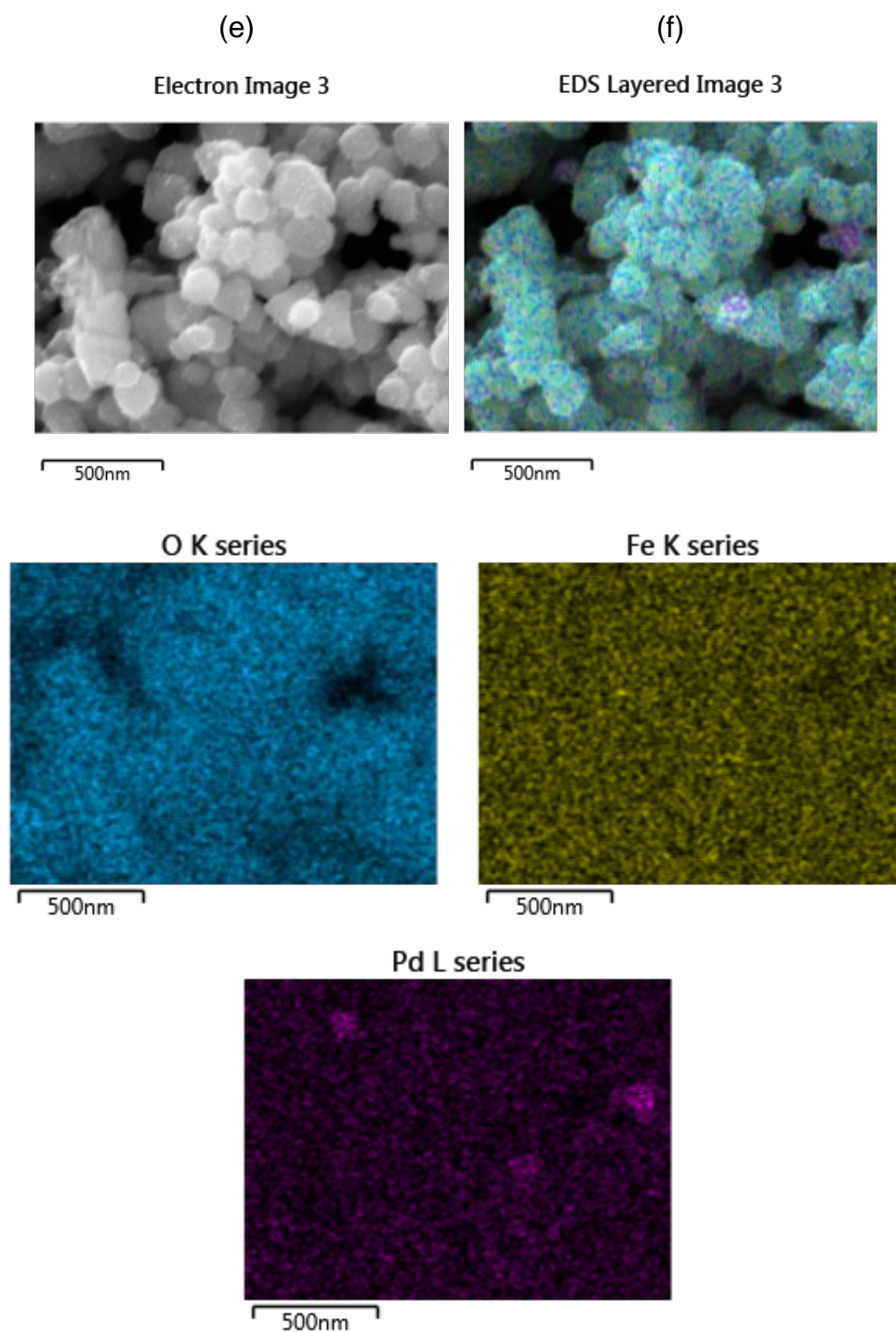
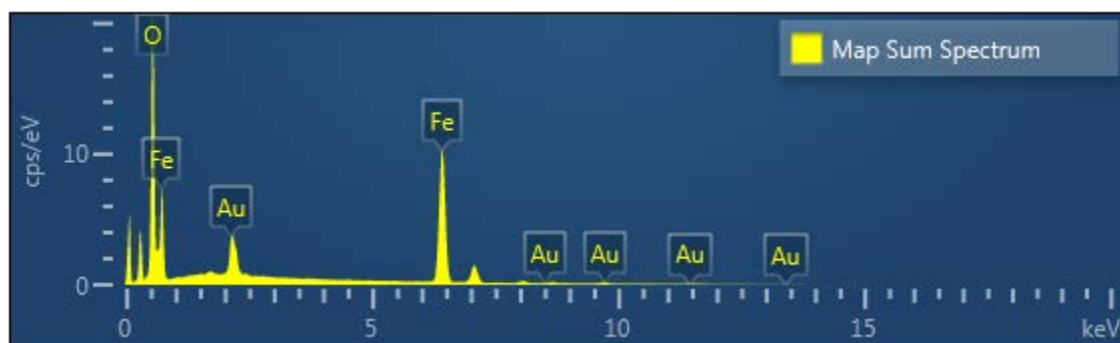
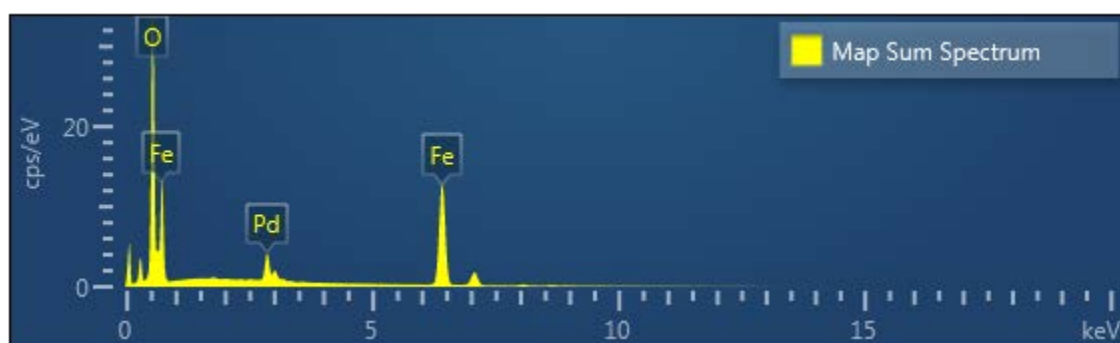


Figure S2. (a) and (b) SEM-EDS images of AuPd-Fe₃O₄ NPs; (c) and (d) SEM-EDS images of Au-Fe₃O₄ NPs; (e) and (f) SEM-EDS images of Pd-Fe₃O₄ NPs

(a)



(b)



(c)

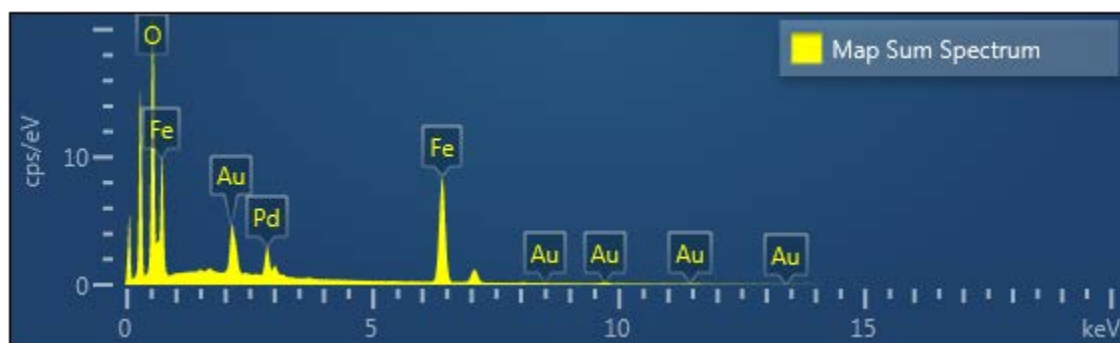
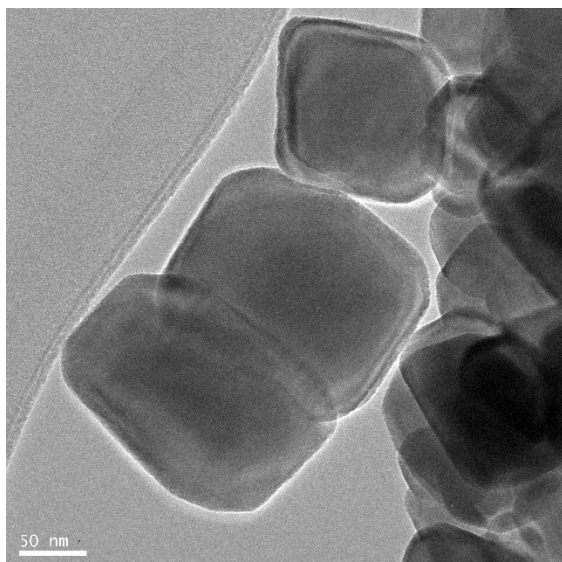
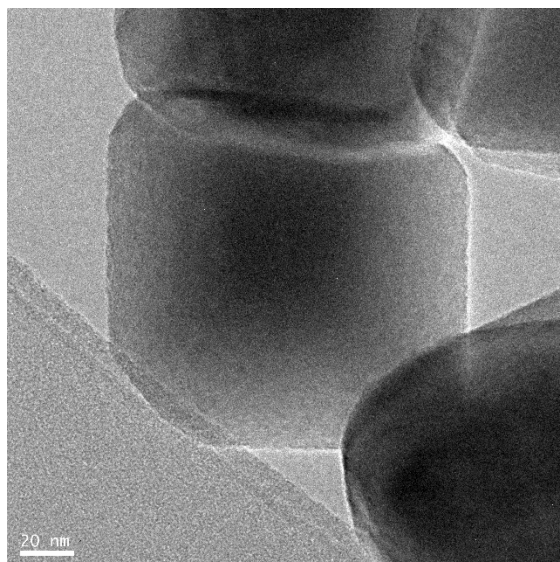


Figure S3. The energy disperse spectroscopy (EDS) map sum spectrum pattern of NPs; (a) Au-Fe₃O₄ NPs, (b) Pd-Fe₃O₄ NPs, and (c) AuPd-Fe₃O₄ NPs

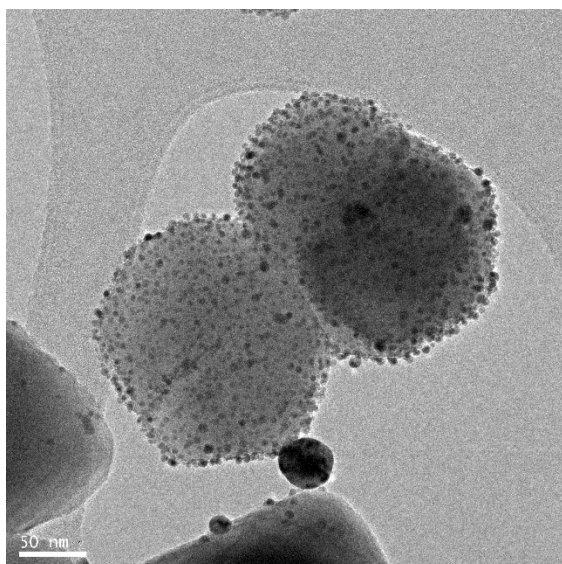
(a)



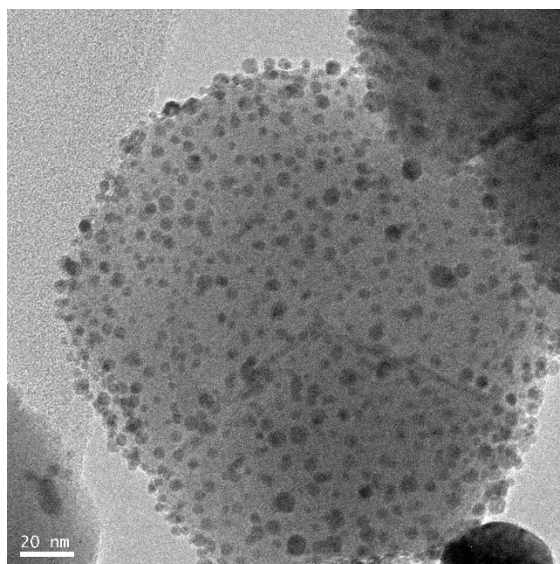
(b)



(c)



(d)



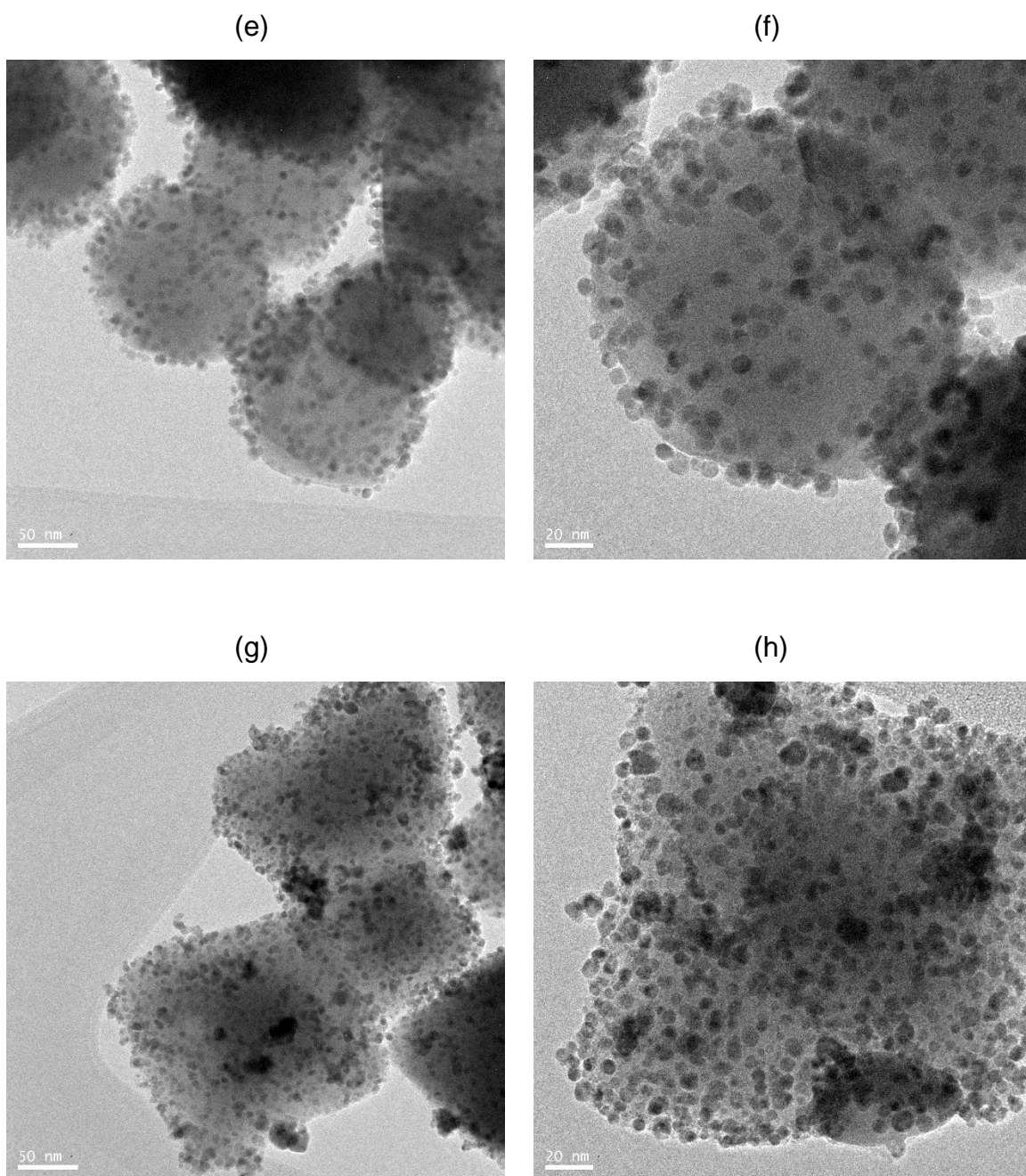
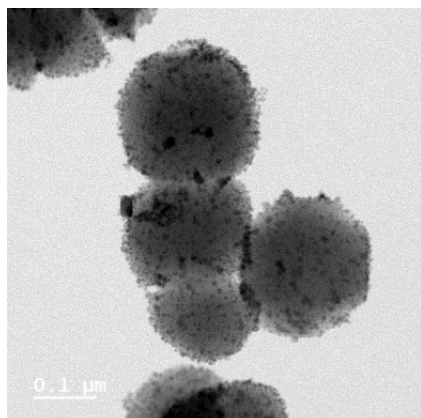
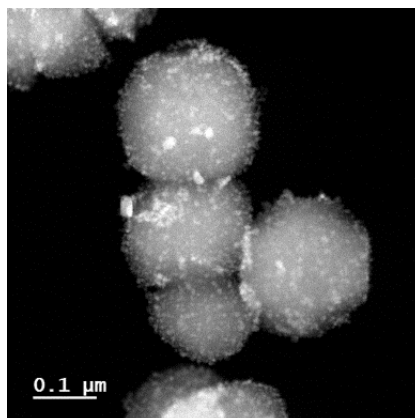


Figure S4. HR-TEM images of (a) and (b) Fe₃O₄ NPs; (c) and (d) Au-Fe₃O₄ NPs; (e) and (f) Pd-Fe₃O₄ NPs; (g) and (h) AuPd-Fe₃O₄ NPs

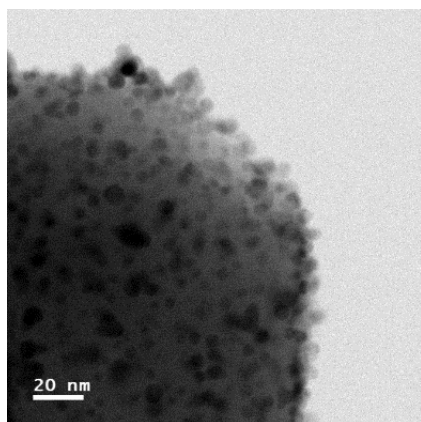
(a)



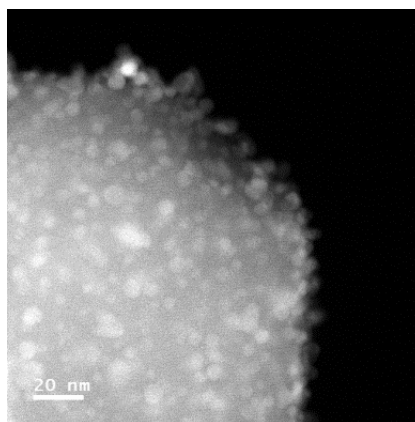
(b)



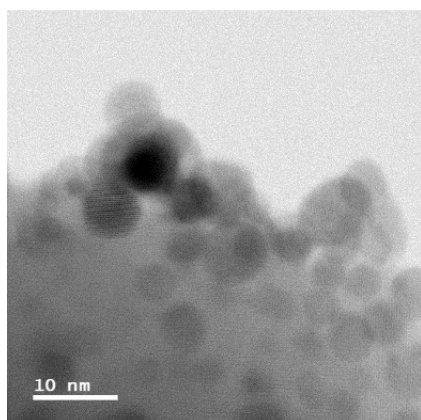
(c)



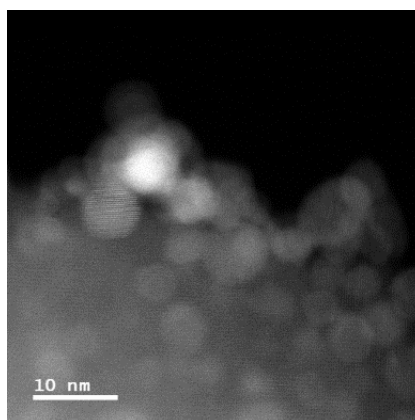
(d)



(e)



(f)



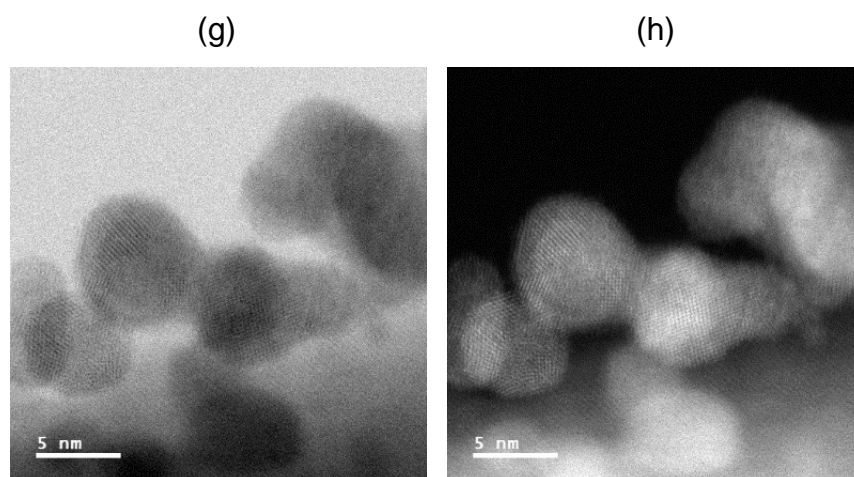
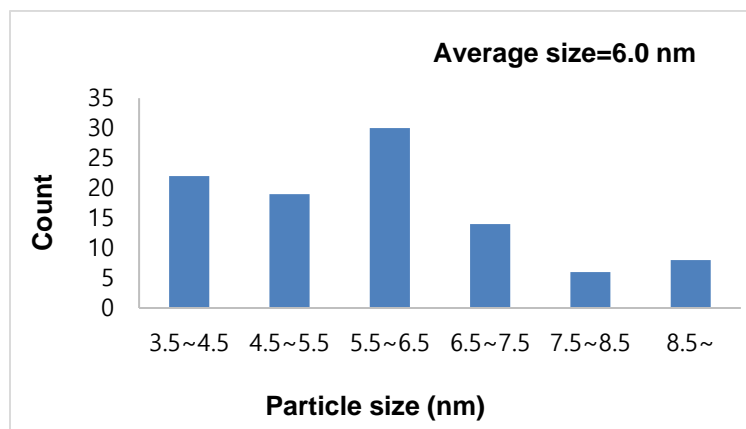
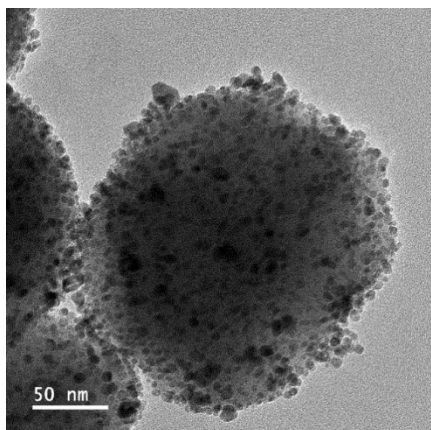
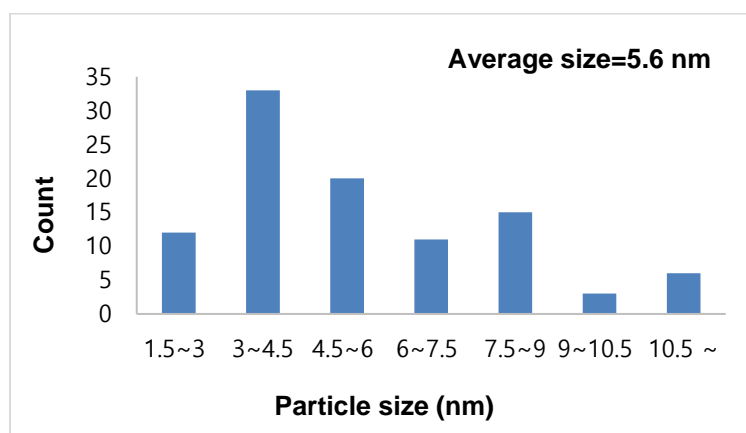
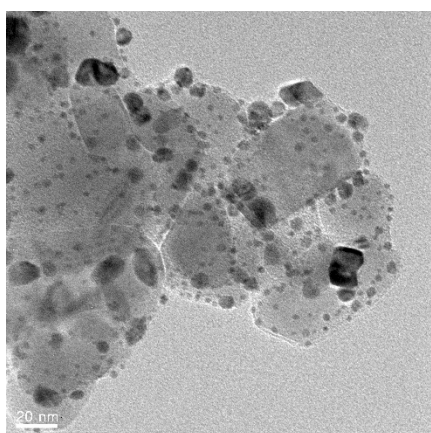


Figure S5. (a), (c), (e), and (g) BF-STEM images of AuPd–Fe₃O₄ NPs; (b), (d), (f), and (h) HADDF-STEM images of AuPd–Fe₃O₄ NPs

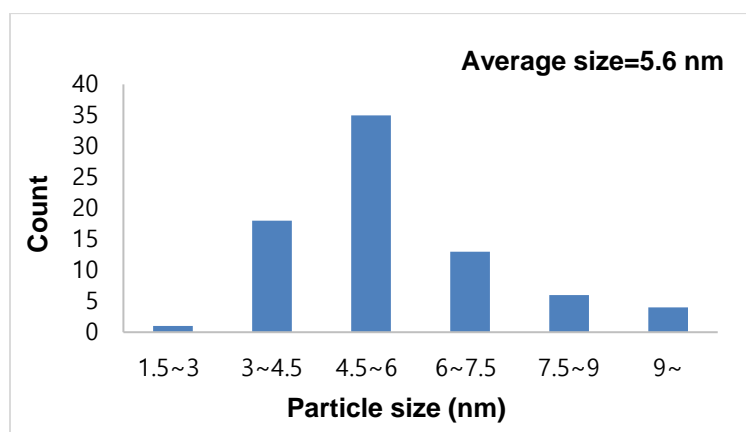
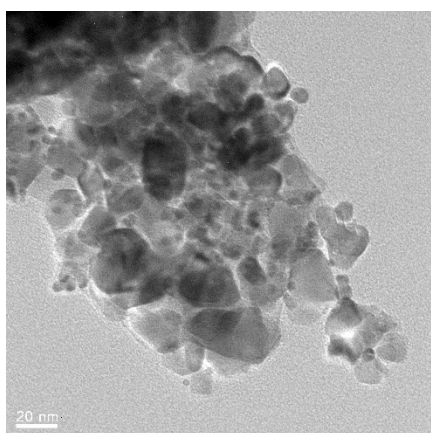
(a)



(b)



(c)



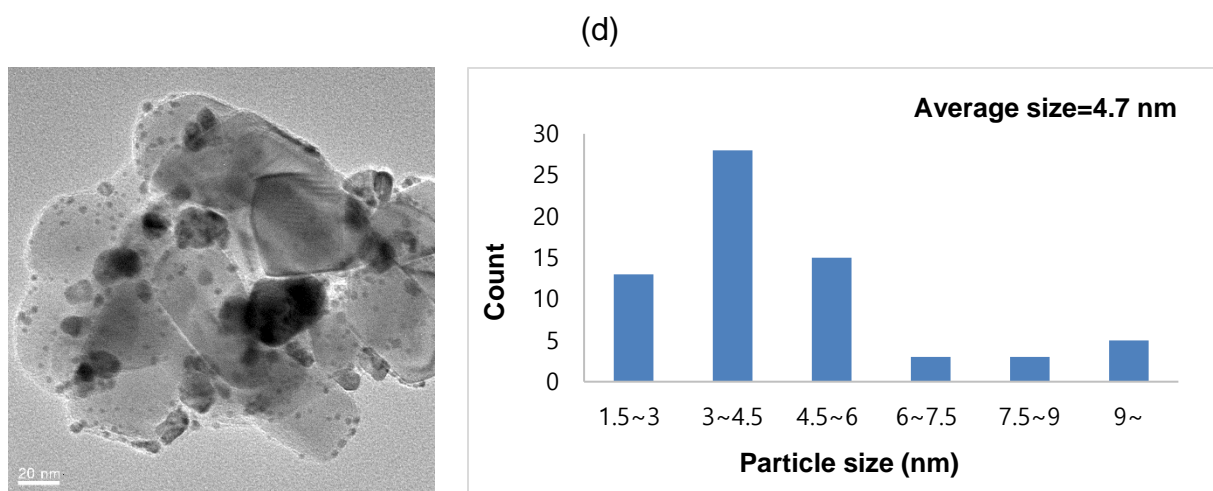
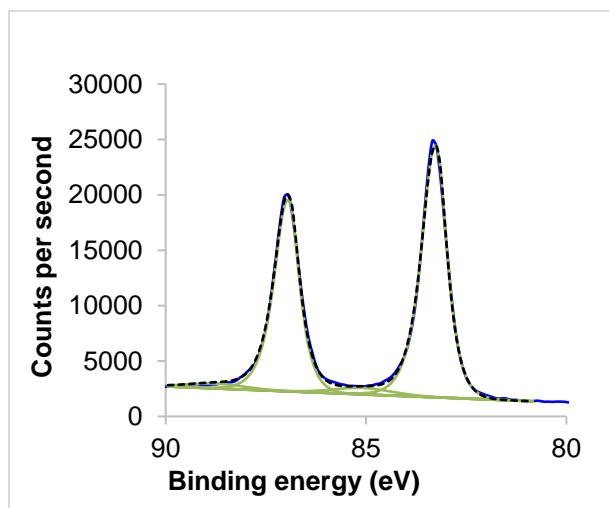
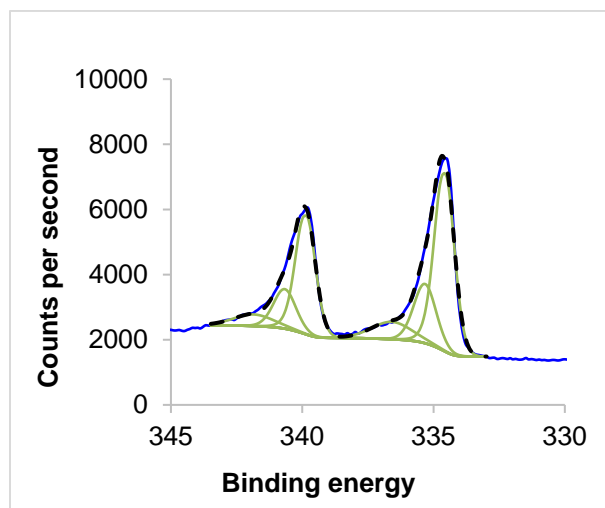


Figure S6. HR-TEM images and particle distribution of (a) AuPd-Fe₃O₄ NPs, (b) AuPd-TiO₂ NPs, (c) AuPd-CeO₂ NPs, and (d) AuPd-C NPs

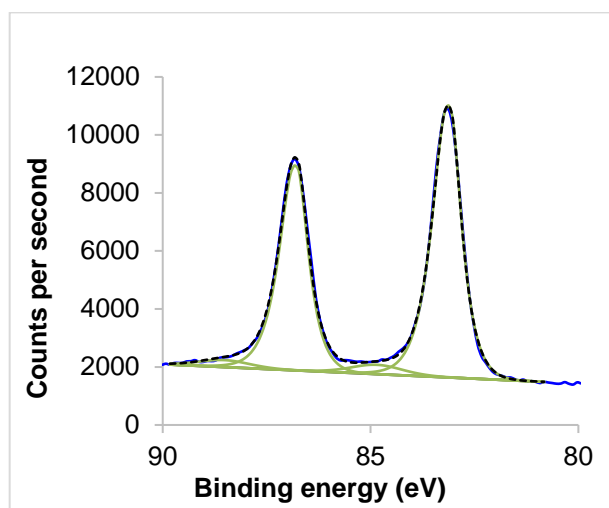
(a)



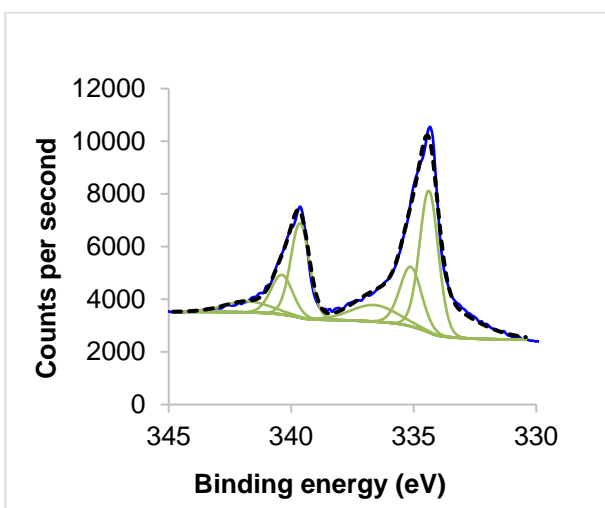
(b)



(c)



(d)



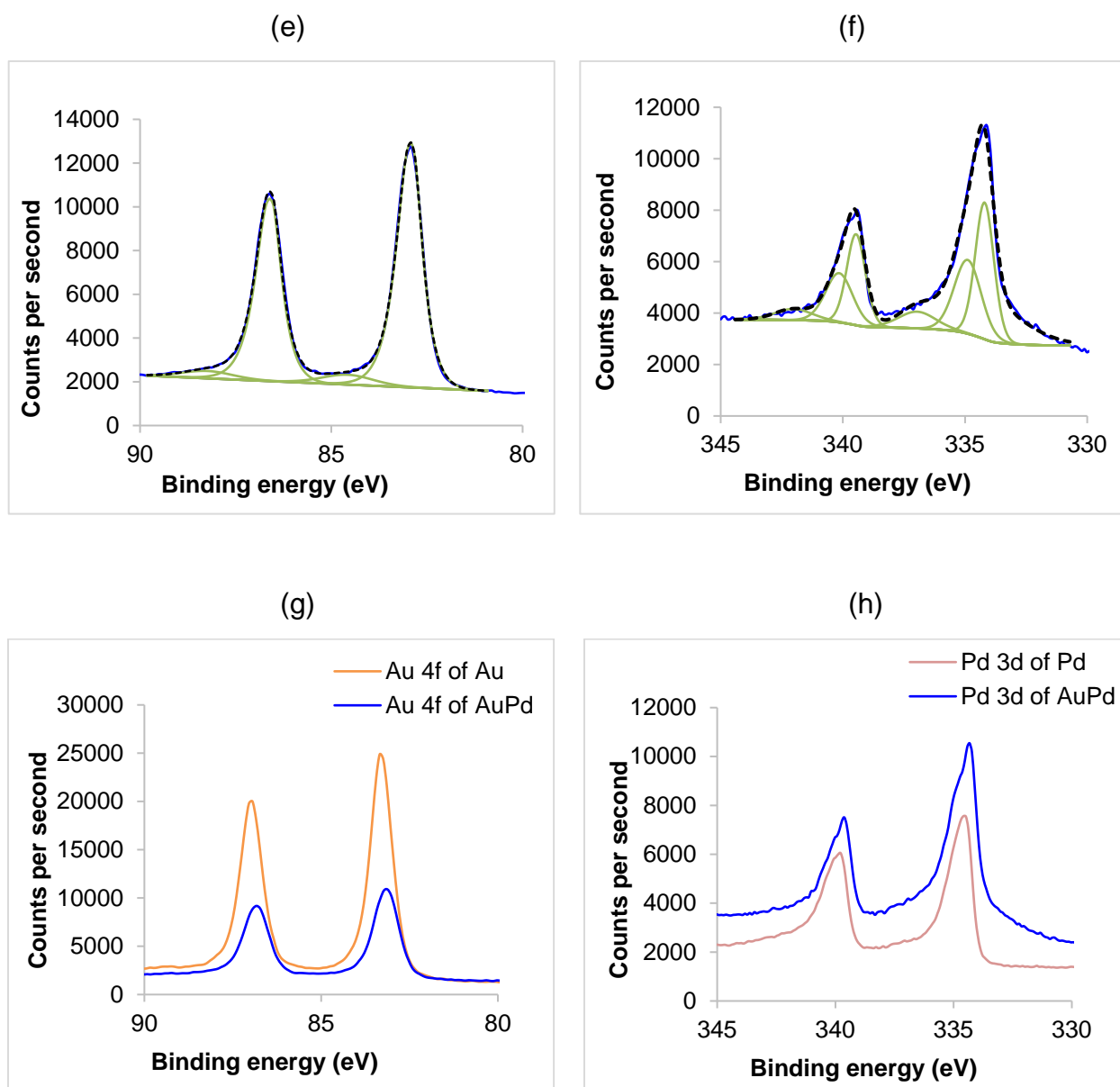


Figure S7. XPS data (a) Au 4f spectra of Au-Fe₃O₄ NPs; (b) Pd 3d spectra of Pd-Fe₃O₄ NPs; (c) Au 4f spectra of fresh AuPd-Fe₃O₄ NPs; (d) Pd 3d spectra of fresh AuPd-Fe₃O₄ NPs; (e) Au 3d spectra of AuPd-Fe₃O₄ NPs after 1 cycle of the catalytic reaction; (f) Pd 3d spectra of AuPd-Fe₃O₄ NPs after 1 cycle of the catalytic reaction; (g) Au 4f spectra of AuPd-Fe₃O₄ NPs and Au-Fe₃O₄ NPs (h) Pd 3d spectra of AuPd-Fe₃O₄ NPs and Pd-Fe₃O₄ NPs

Catalyst	Au (wt%)	Pd (wt%)
AuPd-Fe ₃ O ₄	8.91	5.19
Au-Fe ₃ O ₄	10.5	-
Pd-Fe ₃ O ₄	-	7.52
AuPd-Fe ₃ O ₄ (after 1 st reaction)	8.00	4.18
AuPd-Fe ₃ O ₄ (after 10 th reaction)	4.35	1.89

Figure S8. ICP-AES data of AuPd-Fe₃O₄ NPs, Au-Fe₃O₄ NPs, Pd-Fe₃O₄ NPs, AuPd-Fe₃O₄ NPs after the first reaction, and AuPd-Fe₃O₄ NPs after the 10th reaction

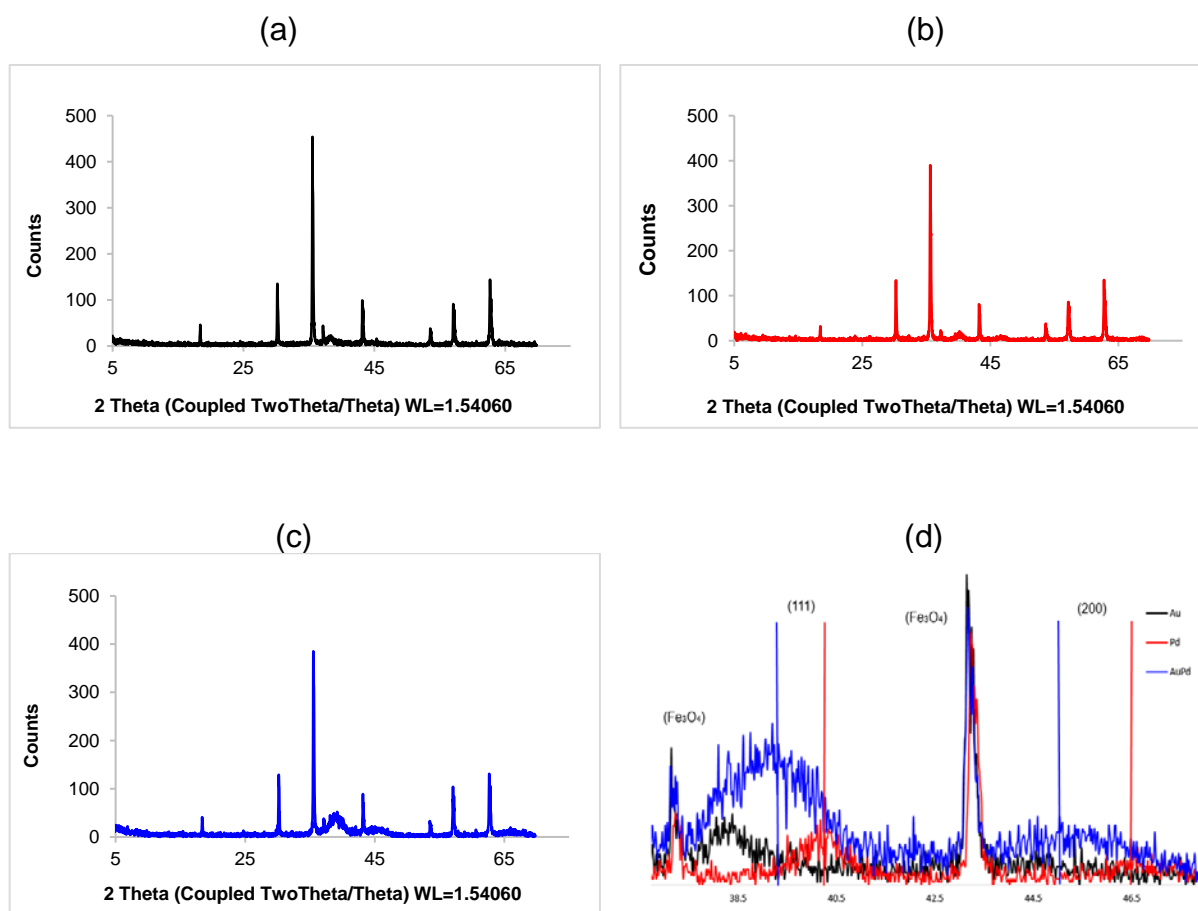
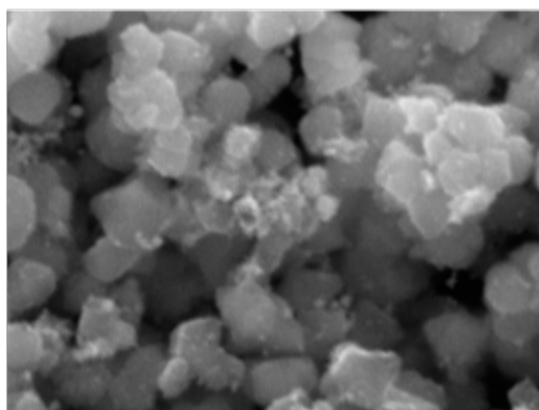


Figure S9. XRD data of (a) Au-Fe₃O₄ NPs, (b) Pd-Fe₃O₄ NPs, (c) AuPd-Fe₃O₄ NPs, and (d) Comparison of XRD peaks of the catalysts

3. Supplementary data

(a)

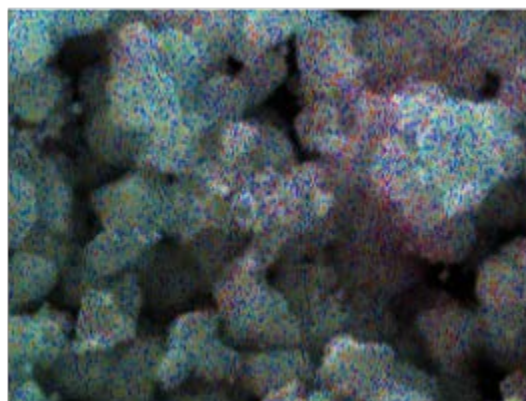
Electron Image 1



500nm

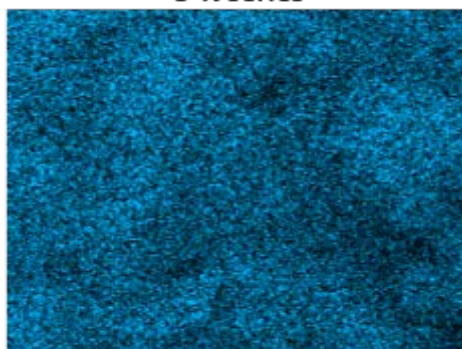
(b)

EDS Layered Image 1



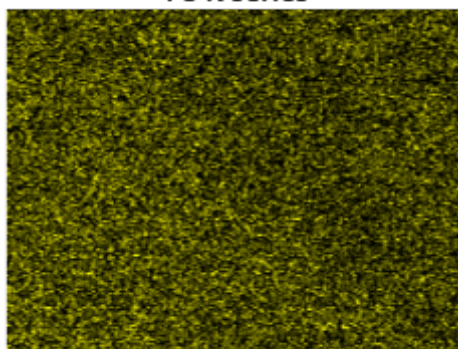
500nm

O K series



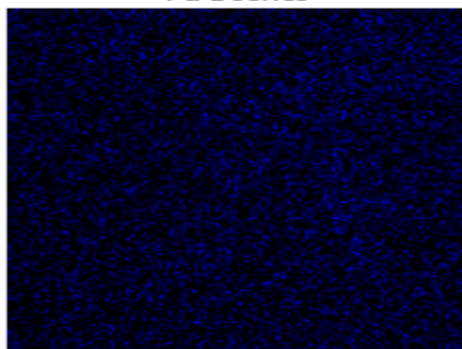
500nm

Fe K series



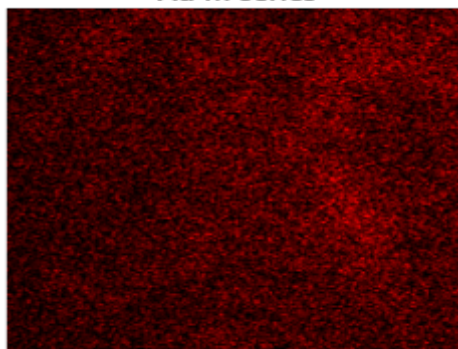
500nm

Pd L series



500nm

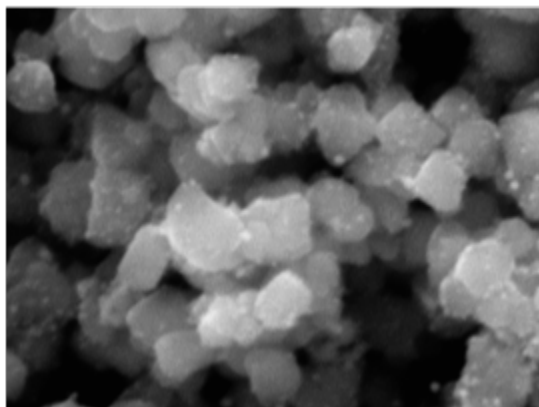
Au M series



500nm

(c)

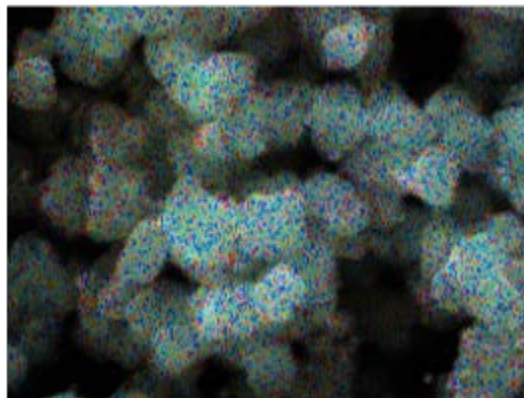
Electron Image 2



500nm

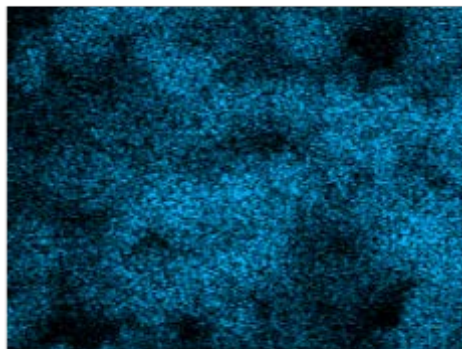
(d)

EDS Layered Image 2



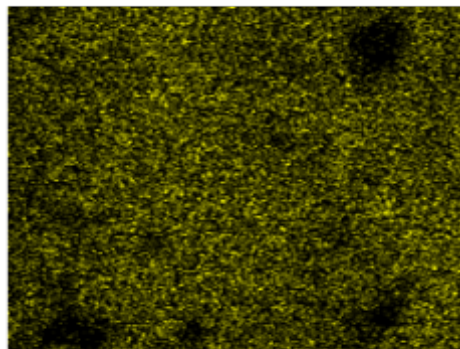
500nm

O K series



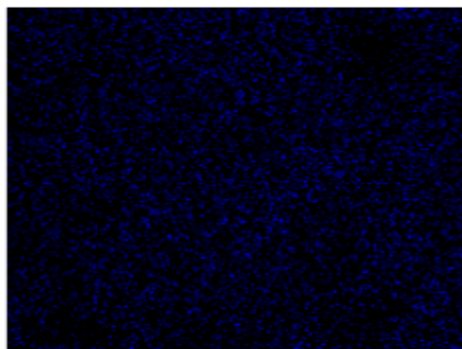
500nm

Fe K series



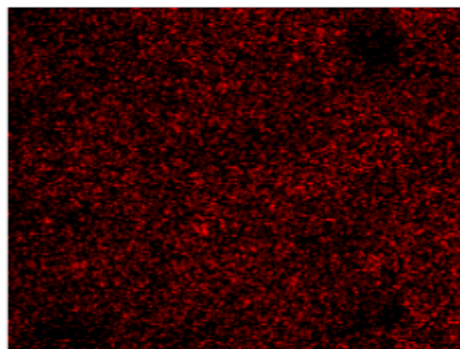
500nm

Pd L series



500nm

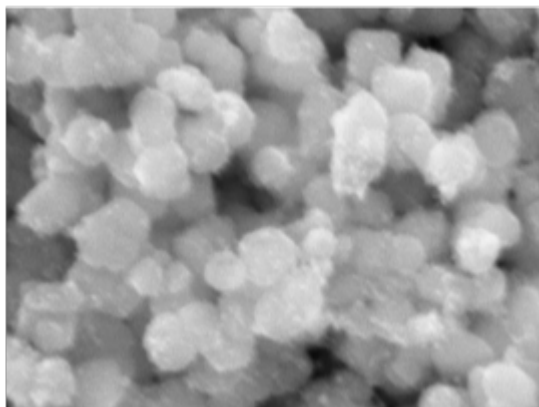
Au M series



500nm

(e)

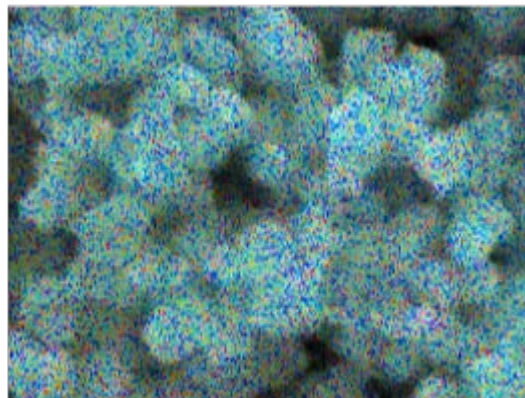
Electron Image 3



7 500nm

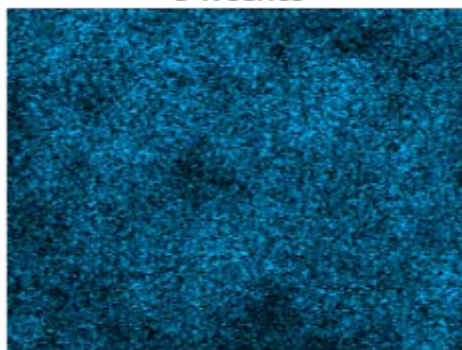
(f)

EDS Layered Image 3



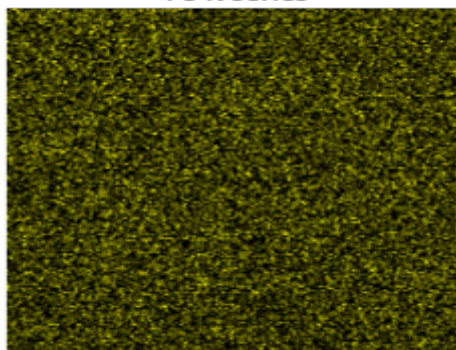
500nm

O K series



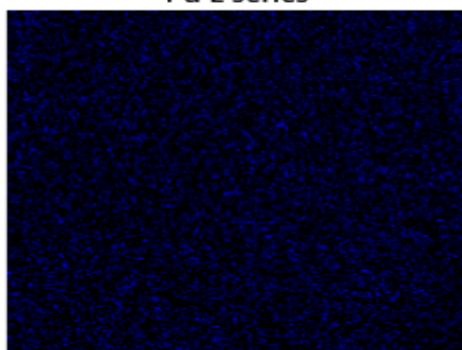
500nm

Fe K series



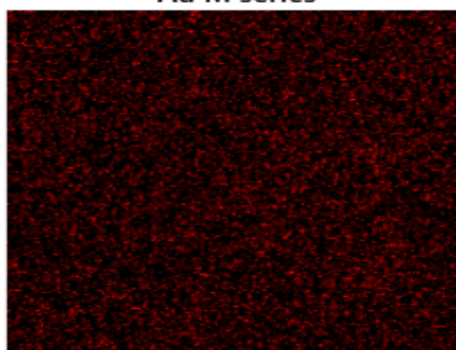
500nm

Pd L series



500nm

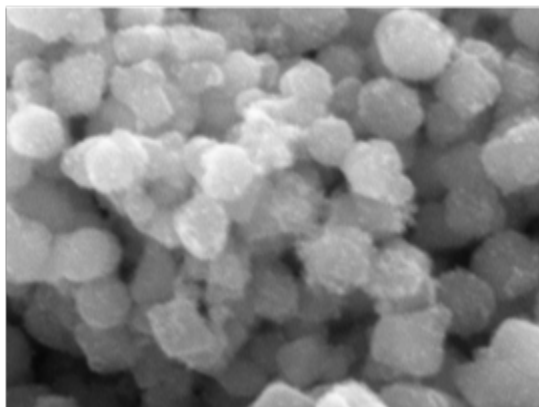
Au M series



500nm

(g)

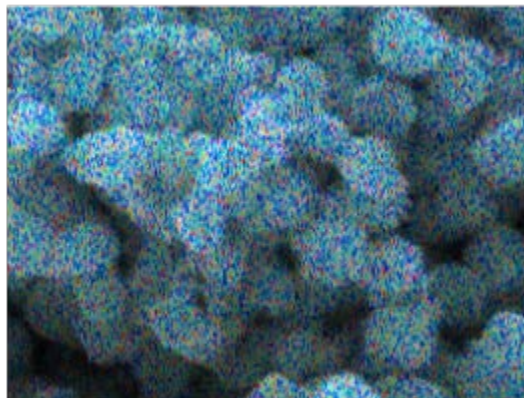
Electron Image 4



500nm

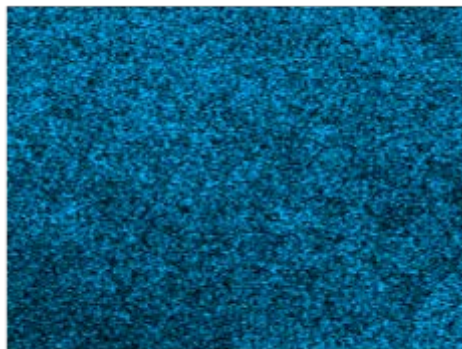
(h)

EDS Layered Image 4



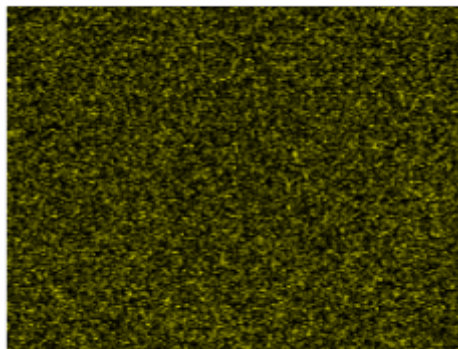
500nm

O K series



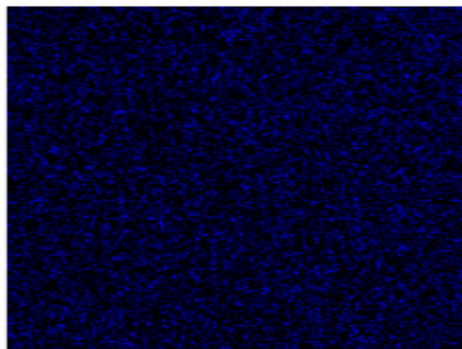
500nm

Fe K series



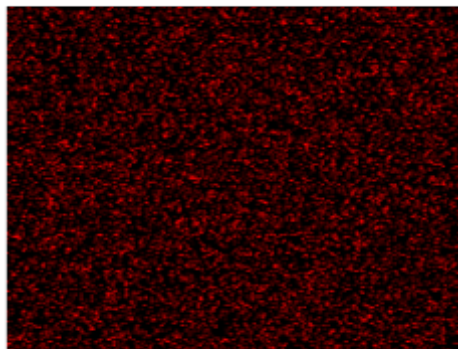
500nm

Pd L series



500nm

Au M series



500nm

(i)

	Au (wt%)	Pd (wt%)	Molar ratio
$\text{Au}_1\text{Pd}_{0.23}\text{-Fe}_3\text{O}_4$	15.1	1.89	1:0.23
$\text{Au}_1\text{Pd}_{0.39}\text{-Fe}_3\text{O}_4$	12.4	2.62	1:0.39
$\text{Au}_1\text{Pd}_{1.08}\text{-Fe}_3\text{O}_4$	8.91	5.19	1:1.08
$\text{Au}_{0.65}\text{Pd}_1\text{-Fe}_3\text{O}_4$	6.54	5.46	0.65:1
$\text{Au}_{0.39}\text{Pd}_1\text{-Fe}_3\text{O}_4$	4.39	6.14	0.39:1

Figure S10. SEM and EDS images of (a) and (b) $\text{Au}_1\text{Pd}_{0.23}\text{-Fe}_3\text{O}_4$ NPs; (c) and (d) $\text{Au}_1\text{Pd}_{0.39}\text{-Fe}_3\text{O}_4$ NPs; (e) and (f) $\text{Au}_{0.65}\text{Pd}_1\text{-Fe}_3\text{O}_4$ NPs; (g) and (h) $\text{Au}_{0.39}\text{Pd}_1\text{-Fe}_3\text{O}_4$ NPs; (i) ICP-AES data of $\text{Au}_x\text{Pd}_y\text{-Fe}_3\text{O}_4$ NPs

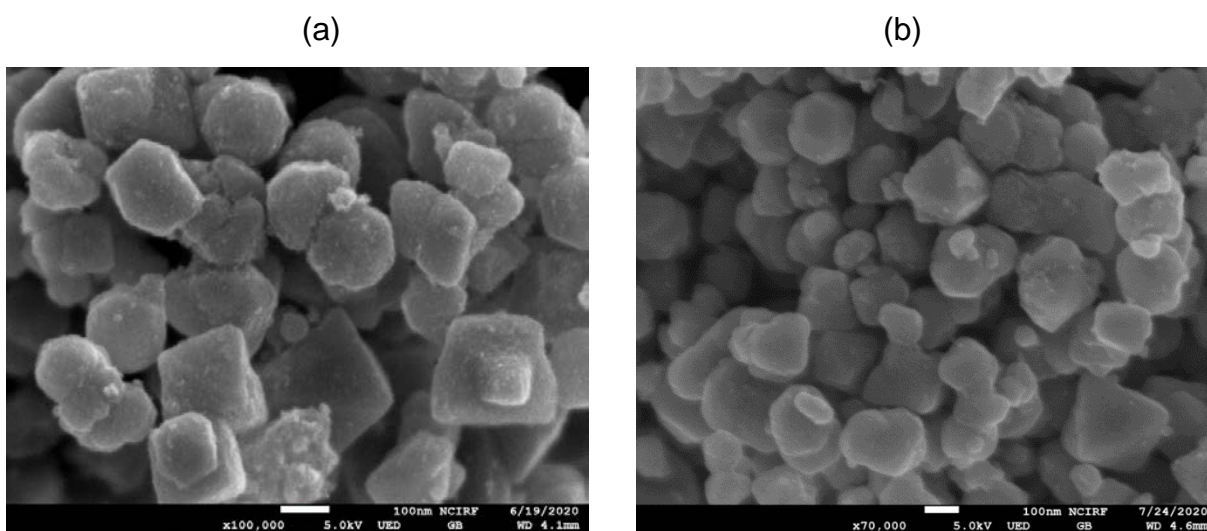


Figure S11. SEM images of $\text{AuPd-Fe}_3\text{O}_4$ NPs after 18 h under 0.50 mmol *N*-methyl-1-phenylmethanamine, 2.4 mol% $\text{AuPd-Fe}_3\text{O}_4$, 3.0 equiv $\text{CsOH}\cdot\text{H}_2\text{O}$ after (a) 1st reaction, (b) 10th reaction

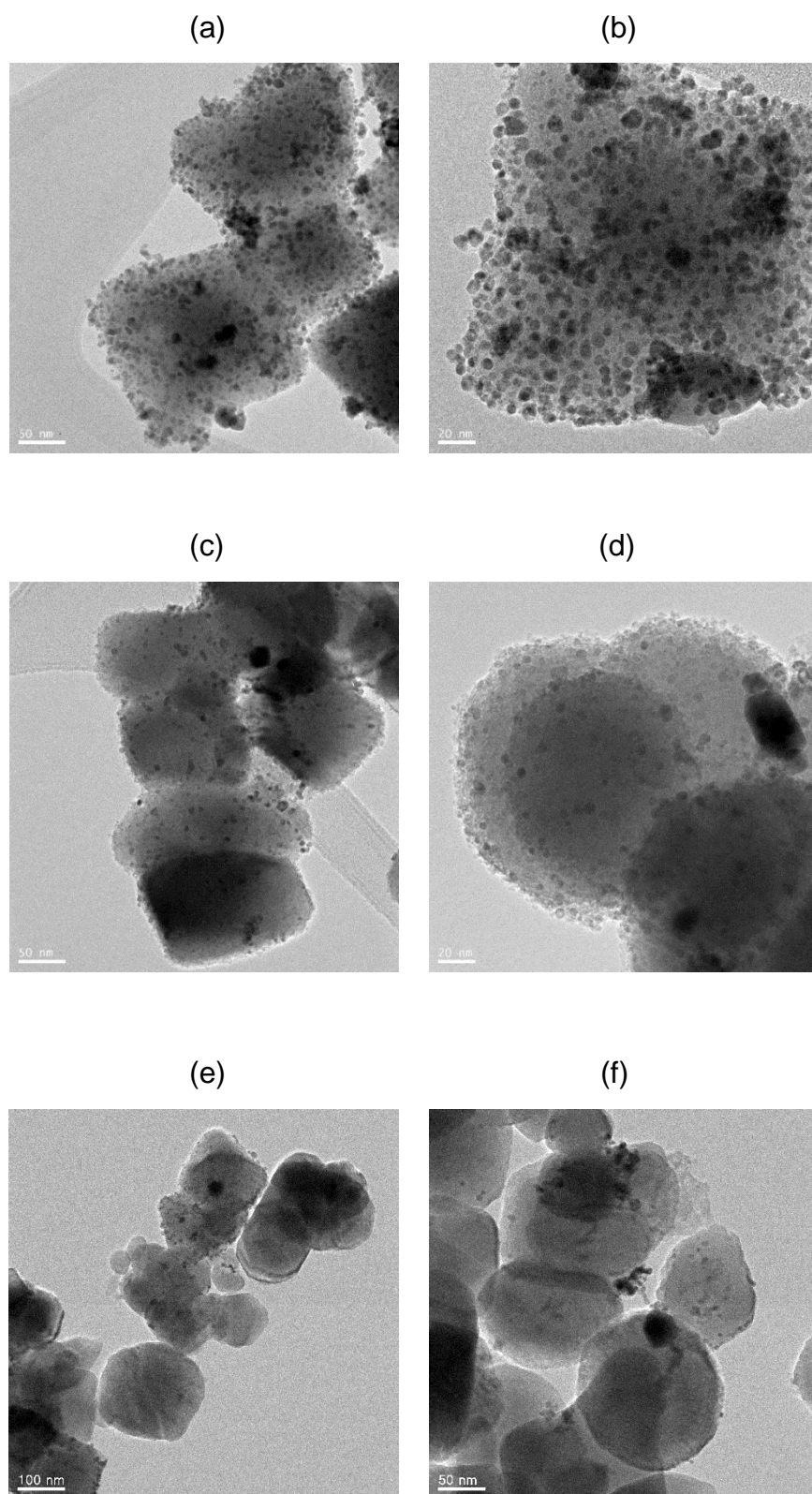


Figure S12. HR-TEM images of (a) and (b) fresh AuPd-Fe₃O₄ NPs; (c) and (d) AuPd-Fe₃O₄ NPs after 1 catalytic cycle; (e) and (f) AuPd-Fe₃O₄ NPs after 10 catalytic cycle

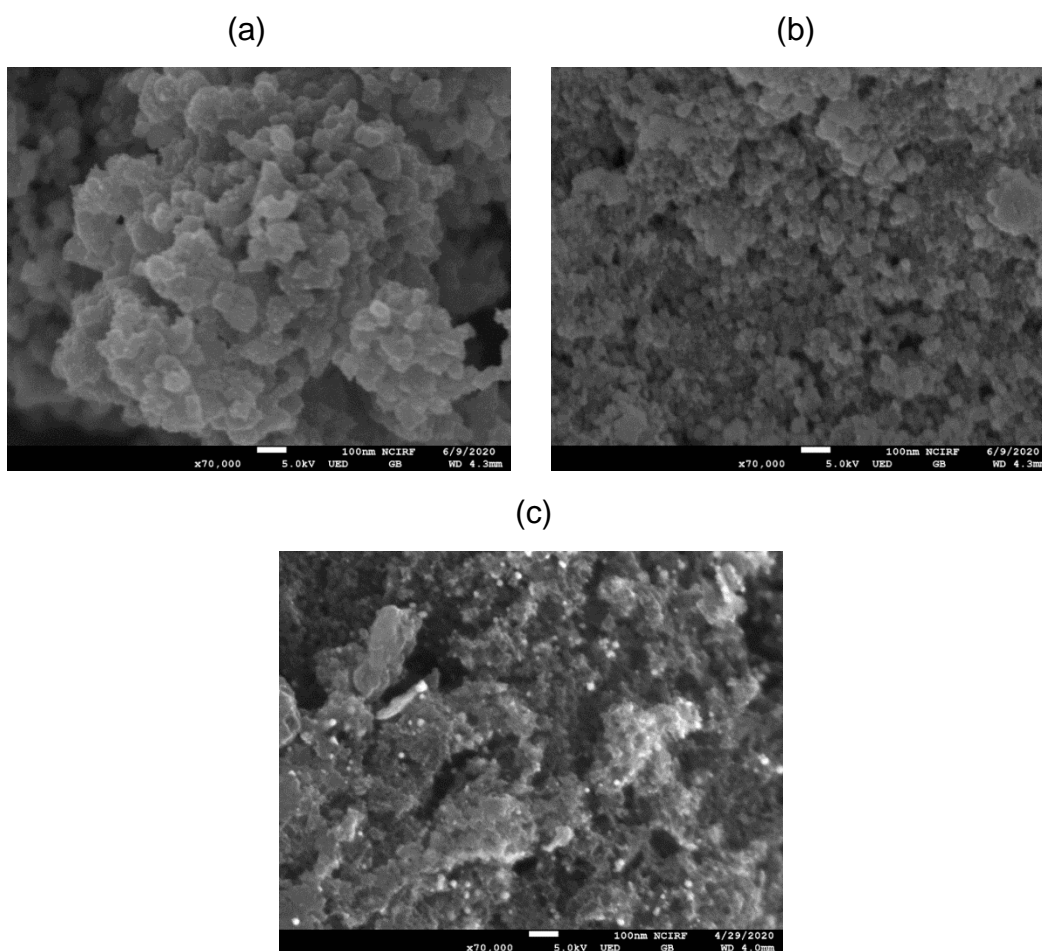


Figure S13. SEM images of (a) AuPd-TiO₂ NPs, (b) AuPd-CeO₂ NPs, and (c) AuPd-C NPs

	Au (wt%)	Pd (wt%)	Au:Pd
AuPd-TiO ₂	10.3	4.51	1:0.81
AuPd-CeO ₂	10.8	5.46	1:0.93
AuPd-C	2.07	1.21	1:1.08

Table S4. ICP-AES data of AuPd NPs with different supports

$ \begin{array}{ccc} \text{Catalyst (1.4 mol\%)} \\ \text{CsOH} \cdot \text{H}_2\text{O (3.0 equiv)} \\ \text{O}_2 \text{ (1.0 atm)} \\ \text{MeOH, r. t., 18 h} \end{array} $			
<chem>CN(C)Cc1ccccc1</chem> 1a (0.20 mmol)	$\xrightarrow{\hspace{1cm}}$	<chem>CN(C)C=O</chem> 2a	
Entry	Catalyst	Au: Pd	Yield (%)
1	AuPd–TiO ₂	1:0.81	55
2	AuPd–CeO ₂	1:0.93	80
3	AuPd–C	1:1.08	48

Table S5. Formylation data of AuPd NPs with different supports

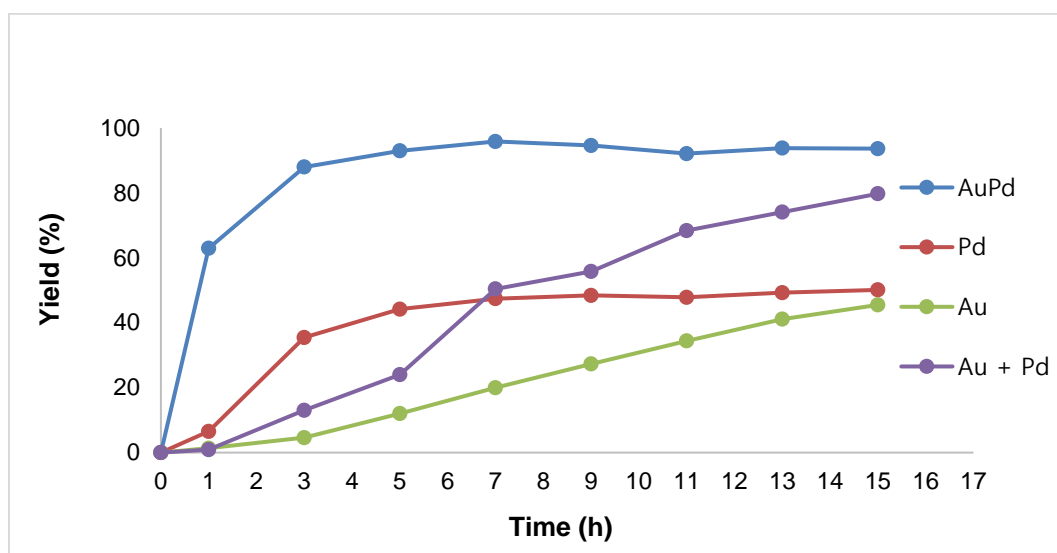
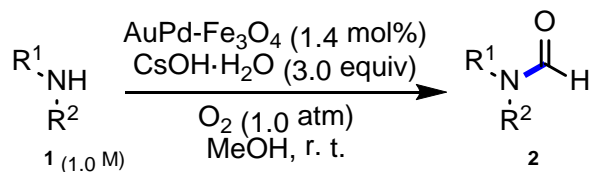


Figure S14. Kinetic data of *N*-formylation of *N*-methyl-1-phenylmethanamine (1.0 mmol scale) with AuPd–Fe₃O₄ NPs (1.4 mol% each of Au and Pd), Au–Fe₃O₄ NPs (2.8 mol%), Pd–Fe₃O₄ NPs (2.8 mol%), and a mixture of Au–Fe₃O₄ NPs (1.4 mol%) with Pd–Fe₃O₄ NPs (1.4 mol%)

Table S6. Substrate scope under high substrate concentration

Entry	Substrate	Yield (%) ^b	Entry	Substrate	Yield (%) ^b
1 ^c	1a	89 ^d (79)	12	1l	78
2	1b	69	13	1m	79
3	1c	83	14	1n	59
4	1d	77	15	1o	22
5	1e	81	16	1p	67
6	1f	73	17	1q	81
7 ^e	1g	87	18	1r	81
8	1h	78	19	1s	9
9	1i	82	20	1t	46
10	1j	76	21	1u	37
11	1k	71			

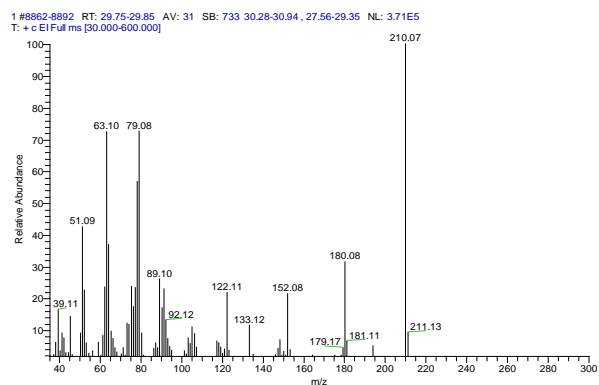
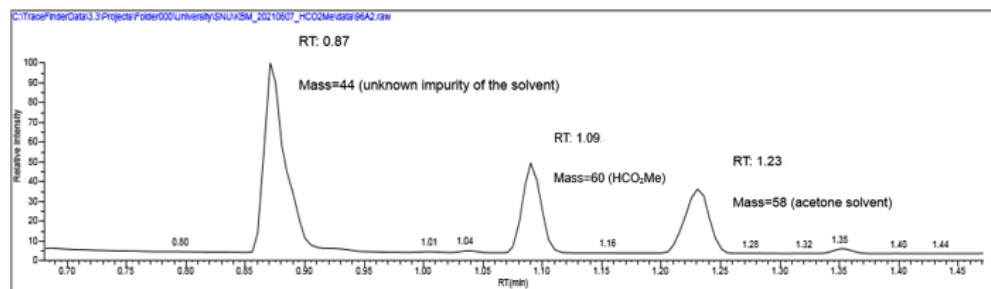
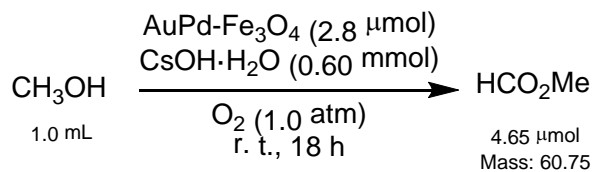
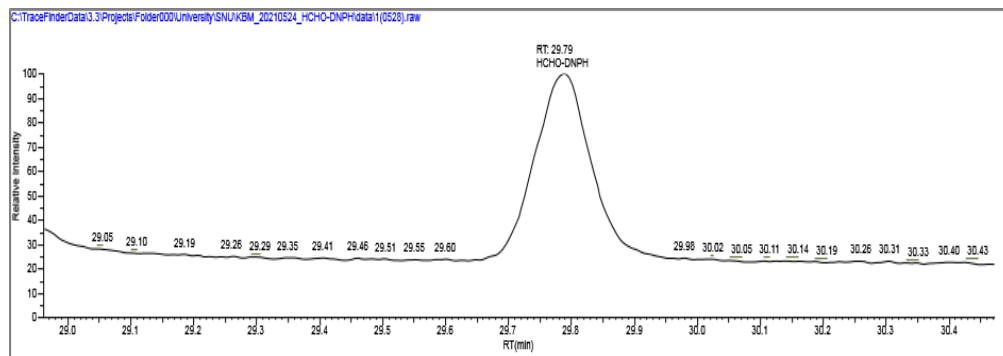
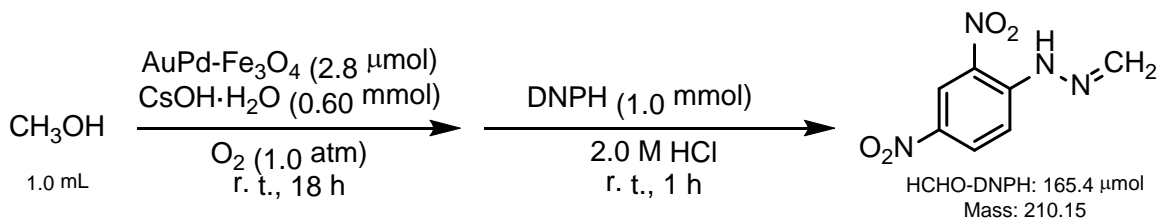
^a Reaction conditions: Amine (1.0 mmol), AuPd-Fe₃O₄ (1.4 mol%), O₂ (1.0 atm), CsOH·H₂O (3.0 equiv), methanol (1.0 mL), r. t., 8 h.

^b Yield of Isolated products.

^c 4 h

^d Determined from ¹H NMR spectral analysis through the use of mesitylene as an internal standard.

^e 6 h



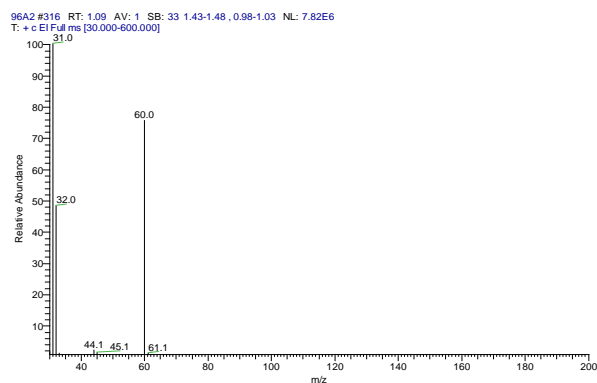


Figure S15. Determination of the methanol oxidation products

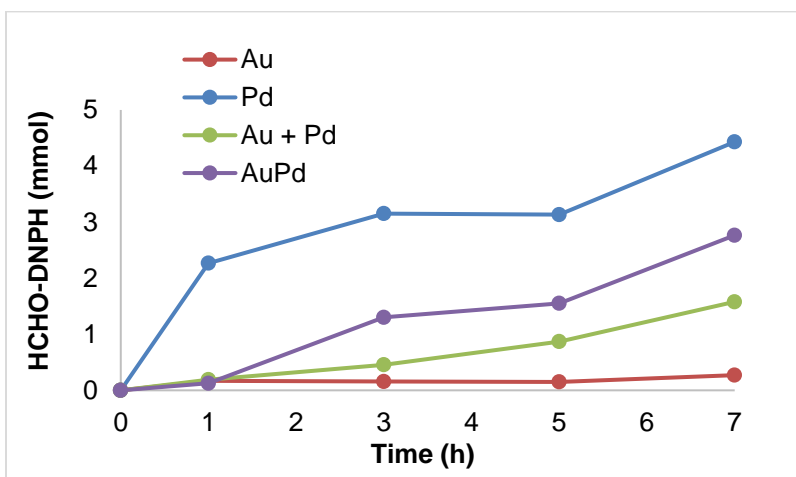
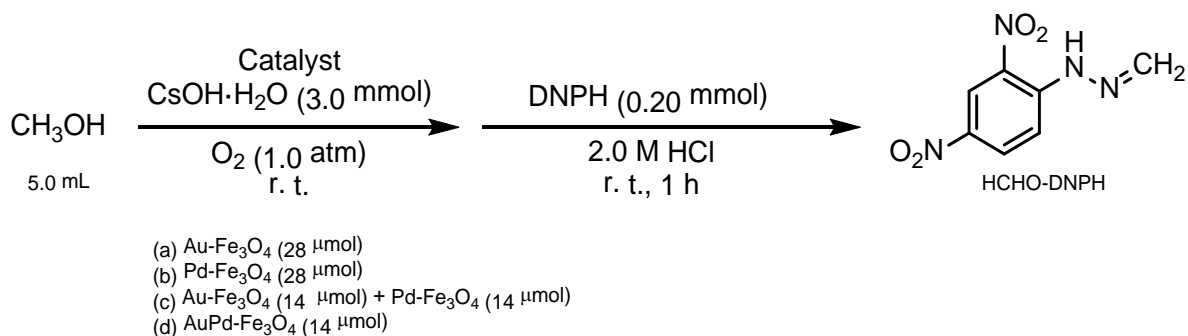
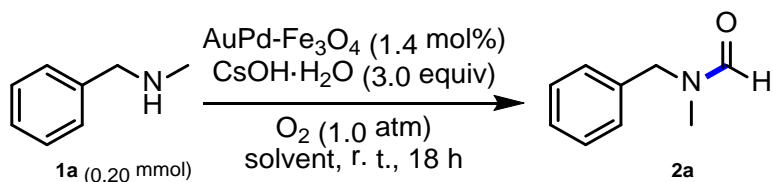


Figure S16. Initial kinetics of methanol oxidation to HCHO as measured from HCHO-DNPH generation

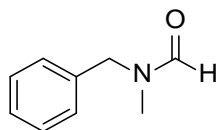
Table S7. Control experiments^a

Entry	Condition	Product yield with the following as a solvent ^b		
		HCHO (37 wt% in H ₂ O)	HCO ₂ H	HCO ₂ Me
1	AuPd	52	< 0.5	71
2	AuPd, CsOH	78	< 0.5	75
3	CsOH	N. D.	N. D.	67

^a *N*-Methyl-1-phenylmethanamine (0.20 mmol), AuPd-Fe₃O₄ (1.4 mol%) CsOH·H₂O (3.0 equiv), solvent (1.0 mL), O₂ (1.0 atm), r. t., 18 h.

^b Determined from ¹H NMR spectral analysis through the use of mesitylene as an internal standard.

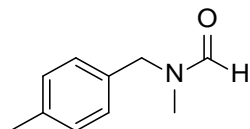
6. Characterization of Products



***N*-benzyl-*N*-methylformamide (2a)**

Yellow oil. The compound was identified by spectral comparison with literature data.^[4]

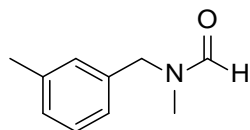
¹H NMR (500 MHz, CDCl₃) δ 8.29 (s, 0.520H, major rotamer), 8.17 (s, 0.380H, minor rotamer), 7.40 – 7.19 (m, 5.00H), 4.53 (s, 0.870H, minor rotamer), 4.40 (s, 1.15H, major rotamer), 2.85 (s, 1.30H, minor rotamer), 2.79 (s, 1.59H, major rotamer). ¹³C NMR (101 MHz, CDCl₃) δ 162.83, 162.67, 136.08, 135.83, 128.97, 128.76, 128.24, 127.71, 127.47, 53.56, 47.84, 34.13, 29.53.



***N*-methyl-*N*-(4-methylbenzyl)formamide (2b)**

Yellow oil. The compound was identified by spectral comparison with literature data.^[5]

¹H NMR (400 MHz, CDCl₃) δ 8.27 (s, 0.620H, major rotamer), 8.14 (s, 0.410H, minor rotamer), 7.21 – 7.11 (m, 3.00H), 7.09 (d, *J* = 7.9 Hz, 1.00H), 4.47 (s, 0.910H, minor rotamer), 4.34 (s, 1.32H, major rotamer), 2.82 (s, 1.40H, minor rotamer), 2.76 (s, 1.83H, major rotamer), 2.34 (d, *J* = 6.5 Hz, 3.00H, mixture of rotamers). ¹³C NMR (101 MHz, CDCl₃) δ 162.75, 162.58, 137.93, 137.39, 133.08, 132.76, 129.62, 129.41, 128.34, 127.46, 53.31, 47.53, 34.03, 29.42, 21.16.

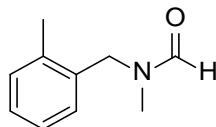


***N*-methyl-*N*-(3-methylbenzyl)formamide (2c)**

Yellow oil.

¹H NMR (400 MHz, CDCl₃) δ 8.28 (s, 0.590H, major rotamer), 8.16 (s, 0.410H, minor rotamer), 7.27 – 7.20 (m, 1.00H), 7.14 – 6.99 (m, 3.00H), 4.48 (s, 0.910H, minor rotamer),

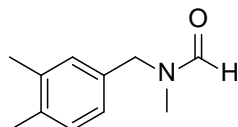
4.35 (s, 1.28H, major rotamer), 2.84 (s, 1.37H, minor rotamer), 2.78 (s, 1.79H, major rotamer), 2.34 (d, $J = 6.5$ Hz, 3.00H, mixture of rotamers). ^{13}C NMR (101 MHz, CDCl_3) δ 162.84, 162.64, 138.78, 138.52, 136.05, 135.81, 129.02, 128.92, 128.86, 128.63, 128.48, 128.13, 125.41, 124.58, 53.54, 47.80, 34.16, 29.56, 21.46. HRMS (ESI) calculated for $\text{C}_{10}\text{H}_{13}\text{NO}$ $[\text{M}]^+$ 163.0997, found 163.0997.



***N*-methyl-*N*-(2-methylbenzyl)formamide (2d)**

Yellow oil.

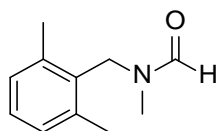
^1H NMR (400 MHz, CDCl_3) δ 8.24 (s, 0.570H, major rotamer), 8.16 (s, 0.420H, minor rotamer), 7.26 – 7.08 (m, 4.00H), 4.54 (s, 0.950H, minor rotamer), 4.40 (s, 1.20H, major rotamer), 2.79 (d, $J = 5.3$ Hz, 3.00H, mixture of rotamers), 2.30 (d, $J = 2.5$ Hz, 3.00H, mixture of rotamers). ^{13}C NMR (101 MHz, CDCl_3) δ 163.06, 162.42, 136.72, 136.19, 133.54, 133.46, 130.84, 130.59, 128.71, 128.07, 127.86, 127.76, 126.37, 126.10, 51.27, 45.62, 34.02, 29.56, 19.18, 19.12. HRMS (ESI) calculated for $\text{C}_{10}\text{H}_{13}\text{NO}$ $[\text{M}]^+$ 163.0997, found 163.1000.



***N*-(3,4-dimethylbenzyl)-*N*-methylformamide (2e)**

Pale yellow oil.

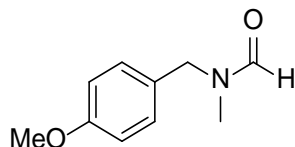
^1H NMR (400 MHz, CDCl_3) δ 8.26 (s, 0.570H, major rotamer), 8.13 (s, 0.370H, minor rotamer), 7.12 – 7.07 (m, 1.00H), 7.03 – 6.90 (m, 2.00H), 4.45 (s, 0.760H, minor rotamer), 4.31 (s, 1.16H, major rotamer), 2.82 (s, 1.22H, minor rotamer), 2.76 (s, 1.68H, major rotamer), 2.24 (d, $J = 6.0$ Hz, 6.00H, mixture of rotamers). ^{13}C NMR (101 MHz, CDCl_3) δ 162.72, 162.53, 137.22, 136.96, 136.50, 135.98, 133.46, 133.15, 130.07, 129.86, 129.60, 128.69, 125.81, 124.93, 53.26, 47.47, 34.02, 29.40, 19.77, 19.73, 19.45. HRMS (ESI) calculated for $\text{C}_{11}\text{H}_{15}\text{NO}$ $[\text{M}]^+$ 177.1154, found 177.1154.



***N*-(2,6-dimethylbenzyl)-*N*-methylformamide (2f)**

Yellow oil.

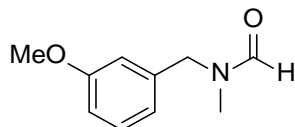
^1H NMR (400 MHz, CDCl_3) δ 8.15 (s, 0.460H, major rotamer), 8.11 (s, 0.430H, minor rotamer), 7.13 (dd, $J = 15.7, 8.8$ Hz, 1.00H), 7.05 (t, $J = 7.1$ Hz, 2.00H), 4.64 (s, 0.980H, minor rotamer), 4.45 (s, 1.07H, major rotamer), 2.72 (s, 1.53H, major rotamer), 2.64 (s, 1.49H, minor rotamer), 2.34 (s, 3.06H, major rotamer), 2.31 (s, 2.88H, minor rotamer). ^{13}C NMR (101 MHz, CDCl_3) δ 162.79, 162.33, 138.15, 137.84, 131.46, 130.82, 128.95, 128.59, 128.41, 128.12, 127.95, 126.78, 53.64, 47.52, 41.25, 40.35, 32.78, 28.84, 20.27, 20.17, 20.10. HRMS (ESI) calculated for $\text{C}_{11}\text{H}_{15}\text{NO}$ $[\text{M}]^+$ 177.1154, found 177.1155.



***N*-(4-methoxybenzyl)-*N*-methylformamide (2g)**

Yellow oil. The compound was identified by spectral comparison with literature data.^[4]

^1H NMR (400 MHz, CDCl_3) δ 8.27 (s, 0.590H, major rotamer), 8.12 (s, 0.410H, minor rotamer), 7.18 (d, $J = 8.3$ Hz, 1.00H), 7.13 (d, $J = 8.4$ Hz, 1.00H), 6.88 (dd, $J = 12.5, 8.4$ Hz, 2.00H), 4.45 (s, 0.870H, minor rotamer), 4.32 (s, 1.18H, major rotamer), 3.80 (d, $J =$ Hz, 3.00H, mixture of rotamers), 2.82 (s, 1.34H, minor rotamer), 2.75 (s, 1.69H, major rotamer). ^{13}C NMR (101 MHz, CDCl_3) δ 162.64, 162.54, 159.50, 159.17, 129.69, 128.82, 128.19, 127.69, 114.31, 114.09, 55.35, 55.33, 53.01, 47.19, 33.96, 29.29.

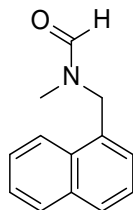


***N*-(3-methoxybenzyl)-*N*-methylformamide (2h)**

Yellow oil.

^1H NMR (400 MHz, CDCl_3) δ 8.20 (s, 0.540H, major rotamer), 8.09 (s, 0.400H, minor rotamer), 7.26 – 7.15 (m, 1.00H), 6.83 – 6.65 (m, 3.00H), 4.43 (s, 0.880H, minor rotamer),

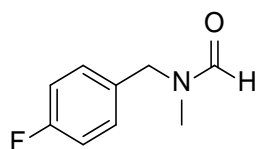
4.30 (s, 1.12H, major rotamer), 3.74 (d, 3.00H, mixture of rotamers), 2.79 (s, 1.43H, minor rotamer), 2.73 (s, 1.60H, major rotamer). ^{13}C NMR (101 MHz, CDCl_3) δ 162.74, 162.56, 160.04, 159.90, 137.59, 137.43, 129.94, 129.66, 120.46, 119.58, 113.67, 113.30, 113.08, 113.03, 55.23, 55.19, 53.37, 47.66, 34.05, 29.45. HRMS (ESI) calculated for $\text{C}_{10}\text{H}_{13}\text{NO}_2$ $[\text{M}]^+$ 179.0946, found 179.0947.



***N*-methyl-*N*-(naphthalen-1-ylmethyl)formamide (2i)**

Yellow oil. The compound was identified by spectral comparison with literature data.^[4]

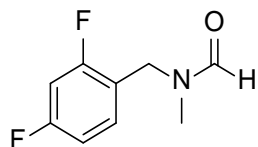
^1H NMR (400 MHz, CDCl_3) δ 8.37 (s, 0.420H, minor rotamer), 8.15 (s, 0.570H, major rotamer), 8.10 – 7.79 (m, 3.00H), 7.58 – 7.27 (m, 4.00H), 4.97 (s, 1.24H, major rotamer), 4.85 (s, 0.830H, minor rotamer), 2.84 (s, 1.20H, major rotamer), 2.72 (s, 1.81H, minor rotamer). ^{13}C NMR (101 MHz, CDCl_3) δ 163.24, 162.35, 133.91, 131.61, 131.38, 131.15, 131.09, 129.11, 128.89, 128.85, 128.71, 127.70, 126.76, 126.72, 126.15, 125.60, 125.38, 125.14, 123.87, 122.34, 51.01, 45.87, 34.01, 30.03.



***N*-(4-fluorobenzyl)-*N*-methylformamide (2j)**

Yellow oil. The compound was identified by spectral comparison with literature data.^[4]

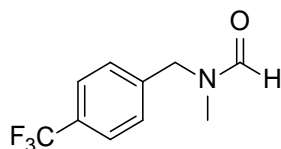
^1H NMR (400 MHz, CDCl_3) δ 8.28 (s, 0.500H, major rotamer), 8.15 (s, 0.450H, minor rotamer), 7.21 (m, 2.00H), 7.04 (m, 2.00H), 4.49 (s, 0.990H, minor rotamer), 4.37 (s, 1.06H, major rotamer), 2.85 (s, 1.45H, minor rotamer), 2.77 (s, 1.49H, major rotamer). ^{13}C NMR (101 MHz, CDCl_3) δ 163.80, 163.56, 162.64 (d, J = 5.6 Hz), 161.34, 161.11, 131.95 (d, J = 3.2 Hz), 131.57 (d, J = 3.2 Hz), 130.02 (d, J = 8.2 Hz), 129.19 (d, J = 8.3 Hz), 116.02, 115.76 (d, J = 7.7 Hz), 115.51, 52.83, 47.12, 34.03, 29.39. ^{19}F NMR (376 MHz, CDCl_3) δ -114.01 – -114.14 (m), -114.72 – -114.87 (m).



***N*-(2,4-difluorobenzyl)-*N*-methylformamide (2k)**

Yellow oil.

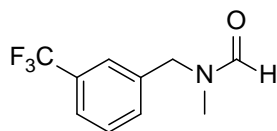
^1H NMR (400 MHz, CDCl_3) δ 8.28 (s, 0.510H, major rotamer), 8.12 (s, 0.460H, minor rotamer), 7.34 – 7.17(m, 1.00H), 6.85 (tdd, J = 18.5, 13.1, 5.2 Hz, 2.00H), 4.55 (s, 0.940H, minor rotamer), 4.42 (s, 1.04H, major rotamer), 2.91 (s, 1.46H, minor rotamer), 2.79 (s, 1.54H, major rotamer). ^{13}C NMR (101 MHz, CDCl_3) δ 164.19, 164.07, 163.77, 163.65, 162.76, 162.71, 162.70, 162.58, 162.45, 162.33, 161.70, 161.59, 161.30, 161.18, 160.09, 159.97, 159.85, 131.74 (dd, J = 9.7, 5.7 Hz), 130.76 (dd, J = 9.8, 5.5 Hz), 111.81 (t, J = 3.7 Hz), 111.60 (t, J = 3.8 Hz), 104.67, 104.41, 104.16, 104.04, 103.78, 103.52, 46.86 (d, J = 3.3 Hz), 40.64 (d, J = 3.3 Hz), 34.23, 29.25 (d, J = 2.0 Hz). ^{19}F NMR (376 MHz, CDCl_3) δ -109.34 – -109.84 (m), -110.35 – -110.48 (m), -114.13 (dd, J = 17.7, 8.7 Hz), -114.69 (dd, J = 17.2, 8.5 Hz). HRMS (ESI) calculated for $\text{C}_9\text{H}_9\text{N}_2\text{O}$ $[\text{M}]^+$ 185.0652, found 185.0649.



***N*-methyl-*N*-(4-(trifluoromethyl)benzyl)formamide (2l)**

Colorless oil. The compound was identified by spectral comparison with literature data.^[4]

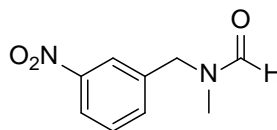
^1H NMR (400 MHz, CDCl_3) δ 8.31 (s, 0.470H, minor rotamer), 8.19 (s, 0.500H, major rotamer), 7.62 (dd, J = 18.5, 8.1 Hz, 2.0H), 7.37 (dd, J = 11.4, 8.3 Hz, 2.0H), 4.58 (s, 1.13H, major rotamer), 4.48 (s, 0.980H, minor rotamer), 2.89 (s, 1.67H, major rotamer), 2.80 (s, 1.37H, minor rotamer). ^{13}C NMR (101 MHz, CDCl_3) δ 162.78, 162.70, 140.27 (d, J = 1.2 Hz), 140.09 (d, J = 1.2 Hz), 130.56, 130.24, 130.06, 129.73, 128.39, 127.68, 125.89 (q, J = 3.8 Hz), 125.65 (q, J = 3.8 Hz), 125.43, 125.31, 122.72, 122.60, 52.93, 47.40, 34.13, 29.54. ^{19}F NMR (376 MHz, CDCl_3) δ -62.62, -62.68.



***N*-methyl-*N*-(3-(trifluoromethyl)benzyl)formamide (2m)**

Colorless oil.

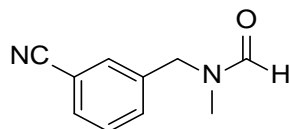
^1H NMR (400 MHz, CDCl_3) δ 8.31 (s, 0.420H, minor rotamer), 8.19 (s, 0.450H, major rotamer), 7.61 – 7.41 (m, 4.00H), 4.58 (s, 1.02H, major rotamer), 4.47 (s, 0.880H, minor rotamer), 2.89 (s, 1.56H, major rotamer), 2.80 (s, 1.30H, minor rotamer). ^{13}C NMR (101 MHz, CDCl_3) δ 162.78 (d, $J = 2.3$ Hz), 137.27, 137.08, 131.60 (d, $J = 1.2$ Hz), 131.30 (d, $J = 1.2$ Hz), 130.99, 130.73 (d, $J = 1.1$ Hz), 129.61, 129.36, 125.39, 125.27, 125.11 (q, $J = 3.8$ Hz), 124.85 (q, $J = 3.8$ Hz), 124.63 (q, $J = 3.8$ Hz), 124.21 (q, $J = 3.8$ Hz), 122.68, 122.56, 53.07, 47.48, 34.19, 29.60. ^{19}F NMR (376 MHz, CDCl_3) δ -62.68, -62.76. HRMS (ESI) calculated for $\text{C}_{10}\text{H}_{10}\text{F}_3\text{NO}$ $[\text{M}]^+$ 217.0714, found 217.0716.



***N*-methyl-*N*-(3-nitrobenzyl)formamide (2n)**

Yellow oil.

^1H NMR (400 MHz, CDCl_3) δ 8.34 (s, 0.390H, minor rotamer), 8.22 (s, 0.720H, major rotamer), 8.20 – 8.11 (m, 2.00H), 7.64 – 7.53 (m, 2.00H), 4.64 (s, 1.24H, major rotamer), 4.54 (s, 0.850H, minor rotamer), 2.94 (s, 1.80H, major rotamer), 2.83 (s, 1.17H, minor rotamer). ^{13}C NMR (101 MHz, CDCl_3) δ 162.85, 162.79, 148.70, 148.52, 138.41, 138.26, 134.29, 133.34, 130.18, 129.93, 123.31, 122.85, 122.84, 122.43, 52.79, 47.30, 34.38, 29.71. HRMS (ESI) calculated for $\text{C}_9\text{H}_{10}\text{N}_2\text{O}_3$ $[\text{M}]^+$ 194.0691, found 194.0690.

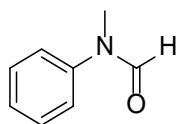


***N*-(3-cyanobenzyl)-*N*-methylformamide (2o)**

Yellow oil. The compound was identified by spectral comparison with literature data.^[6]

^1H NMR (400 MHz, CDCl_3) δ 8.30 (s, 0.390H, minor rotamer), 8.19 (s, 0.560H, major

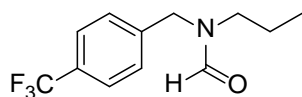
rotamer), 7.67 – 7.44 (m, 4.00H), 4.56 (s, 1.23H, major rotamer), 4.45 (s, 0.890H, minor rotamer), 2.90 (s, 1.80H, major rotamer), 2.80 (s, 1.19H, minor rotamer). ^{13}C NMR (101 MHz, CDCl_3) δ 162.81, 162.74, 137.86, 137.68, 132.65, 131.98, 131.70, 131.57, 131.51, 130.97, 129.99, 129.74, 118.56, 118.32, 113.32, 112.98, 52.77, 47.31, 34.32, 29.70.



***N*-methyl-*N*-phenylformamide (2p)**

Brown oil. The compound was identified by spectral comparison with literature data.^[7]

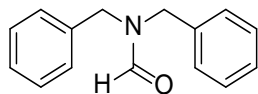
^1H NMR (400 MHz, CDCl_3) δ 8.48 (s, 1.00H), 7.42 (t, J = 7.8 Hz, 2.00H), 7.29 (d, J = 7.4 Hz, 1.00H), 7.18 (d, J = 7.7 Hz, 2.00H), 3.33 (s, 3.00H). ^{13}C NMR (126 MHz, CDCl_3) δ 162.33, 142.19, 129.63, 126.40, 122.36, 32.05.



***N*-propyl-*N*-(4-(trifluoromethyl)benzyl)formamide (2q)**

Colorless oil.

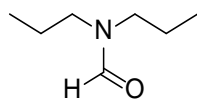
^1H NMR (400 MHz, CDCl_3) δ 8.30 (s, 0.330H, minor rotamer), 8.23 (s, 0.620H, major rotamer), 7.64 – 7.58 (m, 2.00H), 7.39 – 7.34 (m, 2.00H), 4.59 (s, 1.43H, major rotamer), 4.47 (s, 0.670H, minor rotamer), 3.24 – 3.18 (m, 14.0H), 3.14 (t, J = 7.1 Hz, 26.0H), 1.61 – 1.48 (m, 2.00H), 0.90 – 0.86 (m, 3.00H). ^{13}C NMR (101 MHz, CDCl_3) δ 163.10, 163.00, 140.88 (d, J = 1.1 Hz), 140.62, 130.08, 129.76, 128.36, 127.74, 125.94 (q, J = 3.8 Hz), 125.69 (q, J = 3.8 Hz), 125.50, 122.79, 50.81, 48.87, 45.08, 43.85, 21.52, 20.25, 11.30, 10.94. ^{19}F NMR (376 MHz, CDCl_3) δ -62.60, -62.67. HRMS (ESI) calculated for $\text{C}_{12}\text{H}_{14}\text{F}_3\text{NO}$ $[\text{M}]^+$ 245.1027, found 245.1024.



***N,N*-dibenzylformamide (2r)**

Colorless oil. The compound was identified by spectral comparison with literature data.^[8]

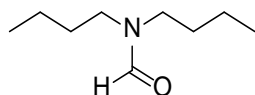
^1H NMR (400 MHz, CDCl_3) δ 8.41 (s, 1H), 7.38 – 7.27 (m, 6.00H), 7.20 – 7.15 (m, 4.00H), 4.41 (s, 2.00H), 4.25 (s, 2.00H). ^{13}C NMR (101 MHz, CDCl_3) δ 162.85, 136.06, 135.69, 128.95, 128.73, 128.54, 128.17, 127.75, 127.69, 50.27, 44.68.



***N,N*-dipropylformamide (2s)**

Yellow oil. The compound was identified by spectral comparison with literature data.^[8]

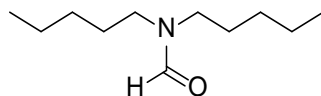
^1H NMR (400 MHz, CDCl_3) δ 8.03 (s, 1.00H), 3.26 – 3.20 (m, 2.00H), 3.14 (t, J = 7.1 Hz, 2.00H), 1.57 – 1.51 (m, 4.00H), 0.88 (td, J = 7.4, 2.6 Hz, 6.00H). ^{13}C NMR (101 MHz, CDCl_3) δ 162.92, 49.27, 43.85, 21.93, 20.64, 11.42, 11.03.



***N,N*-dibutylformamide (2t)**

Yellow oil. The compound was identified by spectral comparison with literature data.^[8]

^1H NMR (400 MHz, CDCl_3) δ 8.04 (s, 1.00H), 3.32 – 3.26 (m, 2.00H), 3.20 (t, J = 7.1 Hz, 2.00H), 1.57 – 1.47 (m, 4.00H), 1.37 – 1.28 (m, 4.00H), 0.98 – 0.91 (m, 6.00H). ^{13}C NMR (101 MHz, CDCl_3) δ 162.76, 47.25, 41.94, 30.83, 29.48, 20.25, 19.73, 13.89, 13.82.



***N,N*-dipentylformamide (2u)**

Yellow oil. The compound was identified by spectral comparison with literature data.^[9]

^1H NMR (400 MHz, CDCl_3) δ 8.04 (s, 1.00H), 3.28 (m, 2.00H), 3.19 (t, J = 7.1 Hz, 2.00H), 1.56 – 1.52 (m, 4.00H), 1.37 – 1.23 (m, 8.00H), 0.93 – 0.88 (m, 6.00H). ^{13}C NMR (101 MHz, CDCl_3) δ 162.74, 47.49, 42.12, 29.15, 28.67, 28.39, 27.04, 22.47, 22.34, 14.05, 14.01.

II. References

- [1] S. Mo, J. Xu, *ChemCatChem* **2014**, 6, 1679.
- [2] M. Takhi, K. Sreenivas, C. K. Reddy, M. Munikumar, K. Praveena, P. Sudheer, B. N.V.M. Rao, G. Ramakanth, J. Sivaranjani, S. Mulik, Y. R. Reddy, K. N. Rao, R. Pallavi, A. Lakshminarasimhan, S. K. Panigrahi, T. Antony, I. Abdullah, Y. K. Lee, M. Ramachandra, R. Yusof, N. A. Rahman, H. Subramanya, *Eur. J. Med. Chem.* **2014**, 84, 382.
- [3] K. Orito, M. Miyazawa, T. Nakamura, A. Horibata, H. Ushito, H. Nagasaki, M. Yuguchi, S. Yamashita, T. Yamazaki, M. Tokuda, *J. Org. Chem.* **2006**, 71, 5951.
- [4] S. Nakai, T. Yatabe, K. Suzuki, Y. Sasano, Y. Iwabuchi, J. Hasegawa, N. Mizuno, K. Yamaguchi, *Angew. Chem. Int. Ed.* **2019**, 58, 16651.
- [5] Z. Liu, Z. Yang, Z. Ke, X. Yu, H. Zhang, B. Yu, Y. Zhao, Z. Liu, *New J. Chem.*, **2018**, 42, 13933.
- [6] T. Yamashita, K. Shiomori, M. Yasuda, K. Shima, *Bull. Chem. Soc. Jpn*, **1991**, 64, 366.
- [7] T. B. Nguyen, J. Sorres, M. Q. Tran, L. Ermolenko, A. Al-Mourabit, *Org. Lett.* **2012**, 14, 3202.
- [8] Z. Ke, Y. Zhang, X. Cui, F. Shi, *Green Chem.*, **2016**, 18, 808.
- [9] J. Li, S. Cai, J. Chen, Y. Zhao, D. Z. Wang, *Synlett* **2014**, 25, 1626.

III. NMR spectra

